The Evaporative Stress Index as an indicator of agricultural drought in Brazil: An assessment based on crop yield impacts

CrossMark

Martha C. Anderson [a,*], Cornelio A. Zolin [b], Paulo C. Sentelhas [c], Christopher R. Hain [d], Kathryn Semmens [e], M. Tugrul Yilmaz [f], Feng Gao [a], Jason A. Otkin [g], Robert Tetrault [h]

[a] USDA-ARS, Hydrology and Remote Sensing Laboratory, Beltsville, MD
[b] Embrapa Agrosilvopastoral, P.O. Box 343, 78550-970, Sinop–MT, Brazil
[c] Department of Biosystems Engineering, ESALQ, University of São Paulo, Piracicaba, SP, Brazil
[d] Earth System Science Interdisciplinary Center, University of Maryland, College Park, MD
[e] Nature Nurture Center, Easton, PA
[f] Middle East Technical University, Civil Engineering Department, Water Resources Division, Ankara, Turkey
[g] Cooperative Institute for Meteorological Satellite Studies, University of Wisconsin-Madison, Madison, WI
[h] USDA Foreign Agricultural Service, Washington, DC

ARTICLE INFO

ABSTRACT

To effectively meet growing food demands, the global agronomic community will require a better understanding of factors that are currently limiting crop yields and where production can be viably expanded with minimal environmental consequences. Remote sensing can inform these analyses, providing valuable spatiotemporal information about yield-limiting moisture conditions and crop response under current climate conditions. In this paper we study correlations for the period 2003–2013 between yield estimates for major crops grown in Brazil and the Evaporative Stress Index (ESI) – an indicator of agricultural drought that describes anomalies in the actual/reference evapotranspiration (ET) ratio, retrieved using remotely sensed inputs of land surface temperature (LST) and leaf area index (LAI). The strength and timing of peak ESI-yield correlations are compared with results using remotely sensed anomalies in water supply (rainfall from the Tropical Rainfall Mapping Mission; TRMM) and biomass accumulation (LAI from the Moderate Resolution Imaging Spectroradiometer; MODIS). Correlation patterns were generally similar between all indices, both spatially and temporally, with the strongest correlations found in the south and northeast where severe flash droughts have occurred over the past decade, and where yield variability was the highest. Peak correlations tended to occur during sensitive crop growth stages. At the state scale, the ESI provided higher yield correlations for most crops and regions in comparison with TRMM and LAI anomalies. Using finer scale yield estimates reported at the municipality level, ESI correlations with soybean yields peaked higher and earlier by 10 to 25 days in comparison to TRMM and LAI, respectively. In most states, TRMM peak correlations were marginally higher on average with municipality-level annual corn yield estimates, although these estimates do not distinguish between primary and late season harvests. A notable exception occurred in the northeastern state of Bahia, where the ESI better captured effects of rapid cycling of moisture conditions on corn yields during a series of flash drought events. The results demonstrate that for monitoring agricultural drought in Brazil, value is added by combining LAI with LST indicators within a physically based model of crop water use.

Published by Elsevier Inc.

1. Introduction

To meet the food supply needs of the world's growing population, global food production will need to roughly double by 2050 (e.g., Global Harvest Initiative, 2014). This increased production must be accomplished within the constraints of a non-uniform distribution of freshwater resources, an amplifying climate cycle, and concern for the environmental impacts of agriculture (Foley et al., 2011). To make significant strides in improving the production capacity and resiliency of global agricultural systems, we must better understand the regional distribution of factors currently limiting production: where crops are most vulnerable to climate extremes, where expansion and intensification can occur with minimal environmental costs, and where infusions of technology in water and land management are likely to significantly improve yields (Lobell et al., 2008; van Ittersum & Cassman, 2013; Zaitchik et al., 2012). Robust early warning indicators highlighting regions with developing crop stress and degrading canopy conditions due to drought

or other stressors are needed to improve within-season yield forecasts and to more effectively mobilize humanitarian response to regional crop failures (Brown, 2008). With an ever-expanding network of earth observing satellites providing free and open data access, remote sensing provides new potential to supply global geospatial information for effective assessments of yield and yield-limiting factors with serviceable spatial and temporal detail.

Remote sensing indicators of agricultural drought convey spatially explicit information regarding variability in water supply (primarily precipitation for rainfed crops), plant available water (soil moisture), crop water requirements and actual water use (evapotranspiration; ET), light-harvesting capacity (green biomass), and crop progress and vegetation health (Basso, Cammarano, & Carfagna, 2013; Rembold, Atzberger, Savin, & Rojas, 2013; Wardlow, Anderson, & Verdin, 2012). An effective large-scale crop monitoring program will require a suite of indicators, because yield limiting factors vary spatially and from year-to-year, and no single indicator will capture all factors. In addition, routine access to multiple indicators facilitates actionable response to drought detection – particularly at the global scale. A convergence of evidence of crop stress emerging in multiple independent yet related indicators leads to greater confidence that the signals are real and that action should be taken. In some cases, one might expect a staged progression of signals through different indicators; for example, a decrease in rainfall leading to crop stress and reductions in ET, and finally manifesting in a degradation in green canopy cover.

One metric of performance for operational drought indicators is a demonstrated linkage to observed impacts on the ground. For agricultural drought, impacts may be most notably manifested in terms of yield reductions. Studies conducted in many countries have investigated correlations between crop yields and spectral vegetation indices (VIs) such as the Normalized Difference Vegetation Index (NDVI; e.g., Becker-Reshef, Vermote, Lindeman, & Justice, 2010; Esquerdo, Júnior, & Antunes, 2011; Fernandes, Rocha, & Lamparelli, 2011; Kogan, Gitelson, Zakarin, Spivak, & Lebed, 2003; Mkhabela, Bullock, Raj, Wang, & Yang, 2011; Mkhabela, Mkhabela, & Mahinini, 2005), the Enhanced Vegetation Index (EVI; Gusso, Ducati, Veronez, Arvor, & da Silveira, 2013; Kouadio, Newlands, Davidson, Zhang, & Chipanshi, 2014), or biophysical parameters like Leaf Area index (LAI; Doraiswamy et al., 2005; Rizzi & Rudorff, 2007; Zhang, Anderson, Tan, Huang, & Myneni, 2005), and fraction of absorbed photosynthetically active radiation (fAPAR; Lobell, Ortiz-Monasterio, Addams, & Asner, 2002; López-Lozano et al., 2015) – all measures of vegetation amount. In addition, landsurface temperature (LST) retrieved from thermal infrared (TIR) remote sensing provides information about temperature extremes encountered during crop development (Gusso, Ducati, Veronez, Sommer, & da Silveira, 2014), as well as stress-induced stomatal closure resulting in elevated canopy temperatures (Jackson, Idso, Reginato, & Pinter, 1981; Moran, 2003). VI- and LST-based indicators have also been combined for yield estimation; with a weighting factor as in the Vegetation Health Index (VHI; Kogan, 1995, 1997; Kogan, Salazar, & Roytman, 2012; Liu & Kogan, 2002; Salazar, Kogan, & Roytman, 2007), through multi-variable regression, decision tree analysis, or other merging criteria (Doraiswamy, Akhmedov, Beard, Stern, & Mueller, 2007; Gusso et al., 2014; Johnson, 2014; Prasad, Chai, Singh, & Kafatos, 2005), or through surface energy balance retrievals of evapotranspiration (ET) – an indicator of vegetation health and soil moisture availability (Bastiaanssen & Ali, 2003; Mishra, Cruise, Mecikalski, Hain, & Anderson, 2013; Tadesse, Senay, Berhan, Regassa, & Beyene, 2015; Teixeira, Scherrer-Warren, Hernandez, Andrade, & Leivas, 2013; Zwart & Bastiaanssen, 2007). Key findings from representative studies comparing VI- and LST-based indicators to crop yields are summarized in Table 1. Other remotely sensed indicators used for yield assessment include solar-induced fluorescence measurements (Guan et al., in press) and microwave retrievals of surface soil moisture (Bolten, Crow, Zhan, Jackson, & Reynolds, 2010).

These studies have investigated both the strength and timing of peak correlations between remote sensing time series and ground-based

yield estimates. Advance signals of anomalous production are beneficial to agricultural producers and commodity markets, and globally for early warning of food insecurity; therefore, earlier peak yield correlations with satellite indicators are a desirable feature. In some climates, responsiveness to rapidly changing conditions is an advantage, such as during rapid onset – or "flash" – drought events. Vegetation health can deteriorate very quickly if moderate precipitation deficits are accompanied by intense heat, strong winds, and sunny skies, as the enhanced evaporative demand quickly depletes root zone moisture (Mozny et al., 2012; Otkin et al., 2013). The ability to pinpoint periods of stress in space and time has motivated assimilation of remote sensing indicators into crop models, which are sensitive to timing of stress within the growing cycle (Ines, Das, Hansen, & Njoku, 2013; Launay & Guerif, 2005; Nearing et al., 2012).

This study assesses the remotely sensed Evaporative Stress Index (ESI) as an indicator of agricultural drought in terms of the timing and magnitude of peak correlations with spatially distributed yield observations. The ESI depicts anomalies in the actual-to-reference ET ratio retrieved via energy balance using remote sensing inputs of LST and LAI (Anderson et al., 2013; Anderson, Hain, Wardlow, Mecikalski, & Kustas, 2011; Anderson, Norman, Mecikalski, Otkin, & Kustas, 2007b). The energy balance scheme incorporates key meteorological variables that drive flash drought, and in the U.S. the ESI has been shown to provide early warning of deteriorating crop moisture conditions in comparison with precipitation or VI-based indices (Anderson et al., 2011, 2013; Otkin et al., 2013; Otkin, Anderson, Hain, & Svoboda, 2014).

The study focuses on the utility of the ESI in explaining regional yield variability in major crops grown in Brazil, which has been identified as an area where significant gains in agricultural production can be achieved, both in terms of expansion and intensification (FAO, 2003). Brazil is a major exporter of several key agricultural products (including soybean, corn, cotton, coffee, sugar and ethanol from sugarcane, and orange juice), and fronts of land use conversion to agriculture continue to expand in the northeast, the central savanna regions (Cerrado), and rainforest transition zones. The north and northeastern states of Maranhão, Tocantins, Piauí and Bahia (the so-called "MATOPIBA" region), for example, are considered a major frontier for new agribusiness investment. However, decisions regarding reasonable expansion are complex and must be informed by analyses of regional climate vulnerability and sustainability of existing ecosystem services. Major droughts in the past decades have severely impacted yields and water availability in some regions of Brazil, particularly in the northeast, pointing to the need for improved drought preparedness in the most climatically vulnerable regions (Gutiérrez, Engle, De Nys, Molejón, & Martins, 2014). This need has led to the recent development of a Northeast Brazil Drought Monitor {http://monitordesecas.ana.gov.br/; \De Nys, 2015 #1142} following the convergence of evidence approach adopted by the U.S. Drought Monitor (Svoboda et al., 2002).

This paper builds on a prior study (Anderson et al., 2015) which compared cross-correlations in ESI with satellite-based precipitation and LAI retrievals and anomalies over Brazil, and their relative behaviors over rainforest vs. agricultural (farm and pasture) land cover classes. Here, these same satellite indicators are compared with a decade of yield data from Brazil, collected between 2003 and 2013. First, the indices are correlated with state-level data for corn, soybean and cotton from the National Food Supply Agency (CONAB), which provides yield estimates discriminated by cropping season (e.g., early vs. late season corn crops). Next, we examine patterns in yield-index correlations at higher spatial resolution using yield estimates at the municipality level from the Brazilian Geographical and Statistical Institute (IBGE). An overarching goal of this study was to evaluate the relative value of different classes of satellite indicators for integration into ongoing drought monitoring, crop modeling and yield estimation efforts in Brazil. We also evaluate the value added by combining LAI – indicative of the VI class of agricultural indicators – with LST in a physically based model of ET, and in comparison with precipitation anomalies

Table 1
Representative studies examining yield correlations with indicators based on remotely sensed LST and VIs combined using (Type 1) weighting factors, (2) regression or decision trees, and (3) integration within a surface energy balance estimate of ET.

Study	Type	RS indicators	Crop	Region	Key findings
Unganai & Kogan (1998)	1	NDVI, LST (AVHRR[1])	Maize	Southern Africa	Stronger index-yield correlations observed where maize is the dominant crop LST correlations peaked in Jan.-Feb. when maize is very sensitive to thermal conditions; NDVI peaked later, attributed to water stress Multiple linear regression using both LST and NDVI indices at their peak correlations were better predictor of yield than either used in isolation
Liu & Kogan (2002)	1	NDVI, LST (AVHRR)	Soybean	8 states in Brazil	For central west and southeast states, LST correlations peaked in Dec.- Jan. (flowering and grain filling); Paraná peaked earlier, Rio Grande do Sul and Santa Catarina later LST generally better predictor of yield than NDVI
Salazar et al. (2007)	1	NDVI, LST (AVHRR)	Winter wheat	Kansas, US	NDVI correlations peak during April–June – critical reproductive period. Earlier correlations (Feb–Mar) with LST, but not as strong as with NDVI
Kogan et al. (2012)	1	NDVI, LST (AVHRR)	Winter wheat, sorghum and maize	Kansas, US	NDVI is a cumulative indicator of crop growth, whereas LST is a state driven by thermal condition and moisture availability. Therefore critical period characterized by LST starts earlier and is shorter than that characterized by NDVI. Sorghum index-yield correlations lower than for maize due to higher drought resistance
Johnson (2014)	2	NDVI, Day/night LST (MODIS), rain	Maize, soybean	US Cornbelt	NDVI and daytime LST were well correlated with yield Nighttime LST and precipitation were not significantly correlated with yield
Gusso et al. (2014)	2	LST, EVI (MODIS)	Soybean	Rio Grande do Sul, Brazil	LST captured occurrences of summer heat stress Optimal correlations (negative) were obtained during grain-filling
Bastiaanssen & Ali (2003)	3	fAPAR (AVHRR), LUE model with ET = f(LST) stress factor	Wheat, rice, cotton, sugarcane	Indus Basin, Pakistan	Model performed satisfactorily for wheat, rice, sugarcane – poorly for cotton 1.1 km resolution of AVHHR too coarse to discriminate individual crops
Mishra et al. (2013)	3	Crop simulation with ET = f(LST), RZ SM updates	Maize	Alabama, US	Remotely sensed actual/reference ET ratio served as reasonable proxy for rootzone soil moisture (RZ SM) from local water balance
Tadesse et al. (2015)	3	ET = f(LST), NDVI, rain	Cereals	Ethiopia	Higher correlation with ET anomalies in northern mountainous region, lower in southern lowlands
This study		ET = f(LST, LAI), LAI, rain	Soybean, corn, cotton	8 states in Brazil	Anomalies in ET ratio (ESI) gave higher and earlier peak correlations with soybean, cotton and first corn crop yields; more uniform index performance for second corn crop ESI outperformed LAI alone, indicating value in combining LAI with LST via energy balance ESI demonstrated fast response to sequence of flash droughts in NE Brazil

[1] Advanced Very High Resolution Radiometer.

that instigate drought. Analyses include assessment of signal convergence between indicators, identification of time windows of maximum sensitivity for each index and crop, and investigation of areas where yield anomalies are well and poorly correlated with ESI in relationship to climatic moisture limitations.

2. Study area

Remotely sensed ET, precipitation and LAI datasets were assembled over a grid with $0.1 \times 0.1°$ (nominally 10×10 km) spatial resolution covering the South American continent (see extent in Fig. 1a). In this study, focus was given to eight major agricultural states in Brazil: Maranhão (MA), Piauí (PI), Bahia (BA), Mato Grosso (MT), Mato Grosso do Sul (MS), Goiás (GO), Paraná (PR), and Rio Grande do Sul (RS). These were selected to represent generalized geographic regions of agricultural production within the northeast, central west and southern parts of Brazil (see Table 2), and were targets of study in Anderson et al. (2015).

A map of land use in Brazil, generated by IBGE based on data from the last agricultural census (2006), is shown in Fig. 1b. The state of MT in the central west represents a transition between tropical forest in the Amazon to the north and a mosaic of agriculture (pasture and crops) and natural savannah (Cerrado) to the south and east. Crops grown in rotation (e.g., soybean, corn and wheat) are most prevalent

in the south and southeast, but are expanding northward as new land is converted to agriculture where climate conditions allow.

3. Data

3.1. Yield data

State-level crop yield datasets were obtained from CONAB (http://www.conab.gov.br/conteudos.php?a=1028), which provides official data on planted area, production and yield back to 1976 for all regions and states in Brazil. The data are collected through survey agents in the agricultural sector, including farmers, cooperatives, secretaries of agriculture, rural extension and financial agents. This work is carried out monthly, with bimonthly field visits supplemented by contacts via phone, electronic mail or other means available for updating the data.

Fig. 2 shows time trends in area planted with soybean, cotton, and first and second season corn crops (denoted "Corn 1" and "Corn 2", with nominal harvest in March and June–July, respectively) over the past decade, as reported by CONAB. State-level planted acreages averaged over the period 2003–2013 are tabulated for each crop in Table 2. Of particular interest is the growth in soybean acreage in MT, in the transitional region from Cerrado to rainforest – nearly doubling between 2002 and 2013 due to recent expansion in a new front of
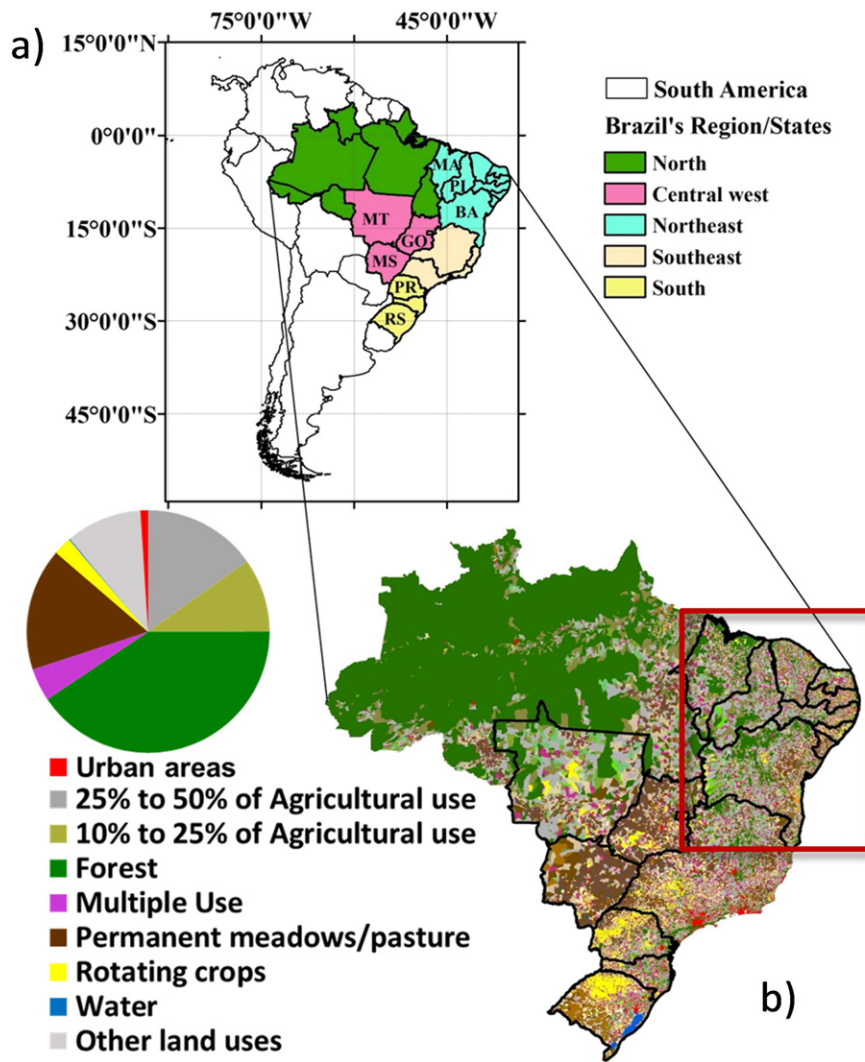
Fig. 1. a) Study region, highlighting regions/states in Brazil used in correlation analyses. Also shown is b) a map of land use over Brazil circa 2006 (IBGE). The red box indicates the northeast region highlighted in Fig. 8. State abbreviations are listed in Table 2.

land occupation. Introduction of new, shorter season (90–100 days) soybean cultivars with reasonable yields has encouraged corn/soybean double-cropping in MT and other states, with soybean being planted at the beginning of the rainy season and an off-season corn crop (safrinha, "Corn 2") at the end of summer. Recent increases in the second corn crop in MT and PR are also due in part to establishment in 2007 of a soybean host-free period ("Vazio Sanitario"), restricting soybean sowing to the first growing season to reduce the occurrence of Asian soybean rust (Delgado & Zanchet, 2011).

To facilitate visualization of sub-state level yield correlations, better approximating the scale of the remote sensing data used in this study, yield estimates were also obtained at the municipality level from the aggregate database from IBGE's Automatic Recovery System (SIDRA; http://www.sidra.ibge.gov.br/), which provides time-series data from 1990 to present aggregated to the country and state level and also at the municipality, district and neighborhood levels. Unlike CONAB, the IBGE dataset does not distinguish yield obtained in different cropping cycles but only provides a bulk annual yield estimate for each crop type.

Table 2
States and regions considered in time series and correlation analyses. Also given are state level estimates of average area planted in soybean, cotton, first and second corn crops (labeled CORN1 and CORN2, respectively) for the period 2003–2013, as well as fraction of total annual corn acreage planted in the second crop (data from CONAB).

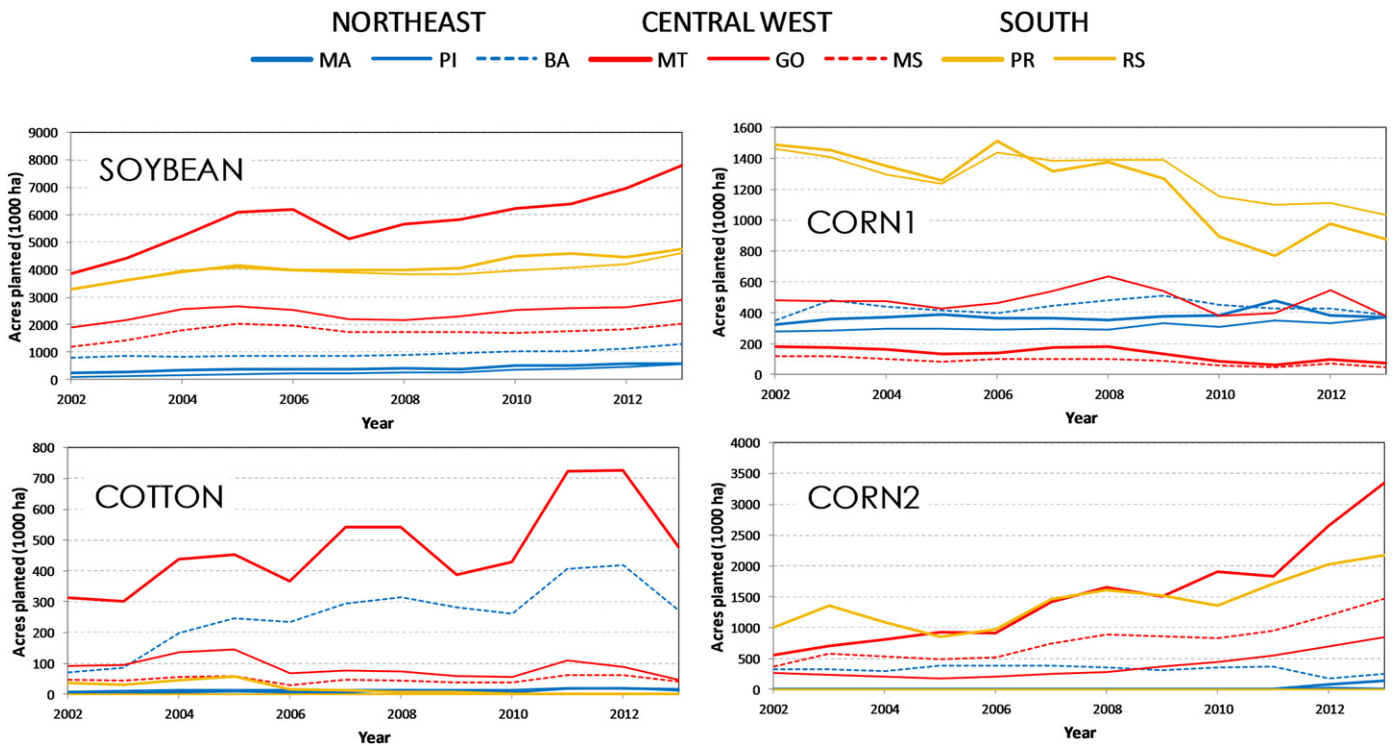| Acronym	State/region	Region	Average planted area (2003–2013) (1000 ha)				
			Soybean	Cotton	Corn 1	Corn 2	Fraction Corn 2
MA	Maranhão	Northeast	430	11	381	19	0.04
PI	Piauí		288	13	313	3	0.01
BA	Bahia		961	274	442	325	0.42
MT	Mato Grosso	Central West	6001	489	128	1607	0.91
MS	Mato Grosso do Sul		1789	47	82	822	0.90
GO	Goiás		2483	86	476	384	0.42
PR	Paraná	South	4183	16	1187	1465	0.55
RS	Rio Grande do Sul		4004	0	1267	0	0.00

Fig. 2. Time trends in planted crop acreage in target Brazilian agricultural states, as reported by CONAB.

While these two yield surveys (IBGE and CONAB) are not completely consistent, they are based on related data sources and exhibit similar magnitudes and tendencies. Discrepancies are generally due to differences in sampling criteria, survey timing (calendar vs. cropping year), and methods for estimating yields at state and national levels (aggregation vs. extrapolation). It is important to note that "yield" is defined in both the CONAB and IBGE datasets as the average ratio of production (kg) per *harvested* area (ha) for each crop, rather than *sowed* area. In some years, crops are so poor that they are not economically viable to harvest, yet this loss of production is not reflected in the reported yields.

Neither IBGE nor CONAB report accuracies associated with their yield estimates. At the country-level, annual production estimates (2001–2014) for corn, soybean, and cotton from CONAB are highly correlated ($r^2 > 0.97$) with World Agricultural Supply And Demand Estimates (WASDE) from the U.S. Department of Agriculture's World Agricultural Outlook Board. However, this does not necessarily constitute an independent assessment due to cross-use of common datasets by both organizations. While we cannot assign error bars to the yield data, it is important to recognize that the observations themselves are an additional source of noise in the correlation analyses.

3.2. Remote sensing data

Remote sensing datasets used in the analyses were described in detail by Anderson et al. (2015), and are summarized briefly below.

3.2.1. Leaf Area Index (LAI)

Daily LAI maps over South America were produced from the 4-day global 1-km MODIS (Moderate Resolution Imaging Spectroradiometer) LAI product (MCD15A3 Terra-Aqua combined, Collection 5). The product was temporally smoothed and gap-filled following the procedures described by Gao et al. (2008) based on the TIMESAT algorithm of Jonsson and Eklundh (2004). The smoothing procedure assigns greater weight to MODIS LAI retrievals with the highest quality, as recorded in the product quality control bits. The final smoothed and gap-filled

time series was then resampled onto the 0.1° analysis grid. Further information is provided by Anderson et al. (2015).

3.2.2. Evapotranspiration (ET)

Maps of daily actual ET were retrieved over the 0.1° analysis grid using a polar orbiter-based version (ALEXI_POLAR; Anderson et al., 2015) of the Atmosphere-Land Exchange Inverse two-source surface energy balance model (Anderson, Norman, Mecikalski, Otkin, & Kustas, 2007a). In this study, ALEXI_POLAR was forced with measurements of day–night LST difference generated using the MODIS-Aqua instantaneous swath product (MYD11_L2), along with insolation and meteorological data from NASA's Modern-Era Retrospective Analysis for Research and Applications (MERRA; Rienecker et al., 2011). The filtered MODIS LAI time series described in Section 3.2.1 is also used as input to ALEXI_POLAR, governing partitioning of surface temperature and fluxes between the soil and canopy components ("sources") in pixels with partial vegetation cover (Kustas & Anderson, 2009).

The Evaporative Stress Index (ESI) is computed from clear-sky estimates of the relative ET fraction, $f_{RET} = ET_a/ET_{ref}$, where ET_a is actual ET retrieved using ALEXI and ET_{ref} is the Penman-Monteith (FAO-56 PM) reference ET for grass as described by Allen, Pereira, Raes, and Smith (1998). Normalizing by reference ET serves to reduce impact of drivers of the evaporative flux that are less directly related to soil moisture limitations (e.g., insolation load and atmospheric demand). To identify areas where f_{RET} is higher or lower than normal for a given time interval within the growing season, ESI is expressed as a seasonally varying standardized anomaly in f_{RET} with respect to long-term baseline conditions. The ESI time-compositing and anomaly computations are described in Section 4.

One limitation of TIR remote sensing is the inability to retrieve LST through cloud cover. This impacts ESI coverage over Brazil during the rainy season, particularly over the Amazon and adjacent states (e.g., MT). Ongoing research is investigating the use of microwave (Ka band) LST retrievals at coarser spatial resolution to supplement TIR retrievals during periods of persistent cloudiness (Holmes, Crow, Hain,

Anderson, & Kustas, 2014); however, in this study TIR-only LST data are used in the ALEXI algorithm.

3.2.3. Precipitation

Daily precipitation grids at 0.25° spatial resolution are routinely available from the Tropical Rainfall Mapping Mission (TRMM) 3B42 v7 precipitation product (Huffman et al., 2007). These rainfall estimates are generated by merging observations acquired at microwave and IR wavelengths. For this study, daily TRMM precipitation estimates were mapped to the 0.1° ALEXI grid using the nearest neighbor resampling.

4. Methods

4.1. Index anomalies

Comparisons between crop yields and satellite indicators were conducted in anomaly space to better focus on changes in yield due to interseasonal climate variability. Standardized anomalies in LAI, TRMM rainfall and clear-sky f_{RET} (i.e., ESI) were computed over relatively short (4 and 12-week, or approximately 1 and 3-month) moving windows, advancing at 7-day timesteps, to identify seasonal/phenological periods where index anomalies are most strongly correlated with harvested yields.

Composites were computed as an unweighted average of all index values over the interval in question:

$$\langle v(w,y,i,j) \rangle = \frac{1}{nc} \sum_{n=1}^{nc} v(n,y,i,j), \tag{1}$$

where v represents LAI, rainfall or f_{RET}, $\langle v(w,y,i,j) \rangle$ is the composite for week w, year y, and i,j grid location, $v(n,y,i,j)$ is the value on day n, and nc is the number of days with good data during the compositing interval. Cloudy-day f_{RET} values from ALEXI_POLAR were flagged and excluded from the composites. This leads to missing data in ESI over the Amazon and surrounding states during the rainy season, particularly between December and February when few clear-sky retrievals are possible. The TRMM and MODIS LAI datasets were completely filled and therefore exhibit no data gaps.

The composited indices were then transformed into a standardized anomaly or "z-score", normalized to a mean of zero and a standard deviation of one. Fields describing "normal" (mean) conditions and temporal standard deviations at each pixel were generated for each compositing interval over the baseline period 2003–2013. Then standardized anomalies at pixel i,j for week w and year y were computed as

$$v(w,y,i,j)' = \frac{\langle v(w,y,i,j) \rangle - \frac{1}{ny} \sum_{y=1}^{ny} \langle v(w,y,i,j) \rangle}{\sigma(w,i,j)}, \tag{2}$$

where the second term in the numerator defines the normal field, averaged over all years ny, and the denominator is the standard deviation. In this notation, f_{RET}' computed for an X-month composite is referred to as ESI-X, where X is 1 or 3 in this study. Anomalies in X-month composites of MODIS LAI and TRMM precipitation are denoted LAI'-X and TRMM'-X, respectively.

4.2. Yield correlations

To assess correlations with state- and municipality-based crop yield estimates, spatially aggregated satellite index anomalies were computed from f_{RET}, LAI and TRMM data averaged over polygons outlining each yield measurement unit, excluding pixels that were not identified as majority agricultural land use as defined in the land cover classification shown in Fig. 1b.

Yield anomalies at both state and municipal levels were computed as departures from a linear regression in time over the 2003–2013 period to remove trends in increasing yield that may result from technological advances or genetic improvements in cultivars:

$$yield(u,y)' = yield(u,y) - yield_{lin}(u,y) \tag{3}$$

where u is the political unit in question (state, region or municipality), y is the year, and $yield_{lin}$ is given by a linear temporal fit to all yield data for that unit over the period of record. Linear detrending of yields may not be appropriate for all states, but in general served to increase correlations with all drought indicators examined.

Index-yield correlations were quantified using the Pearson correlation coefficient (r), typically computed from $ny \times ns$ samples, where $ny = 11$ is the number of years of yield data included in the analysis (2003–2013), and ns is the number of states/municipalities included in a regional evaluation. A Spearman rank correlation provided qualitatively similar results (not shown).

For state-level yield analyses, correlations were computed at 7-day intervals between the 1-month composited index standardized anomalies (Eq. (2)) and yield anomalies (Eq. (3)). To identify optimal windows during the growing season where an index is most predictive of at-harvest yield, a two-dimensional correlation space was computed for each index, crop and region. The 1-month index composites were further averaged over a variable window prior to correlation with yield anomalies. In 2-D plots of these analyses, the x-axis represents the end-date of the index averaging window, and the y-axis represents the length of the window.

Yield correlations at the municipal level were computed at 7-day intervals using 3-month composite drought indices to investigate how date and magnitude of maximum correlation strength vary spatially across the country.

5. Results

5.1. State-level yield correlations

5.1.1. Satellite index and yield time-series

Time-series of ESI, TRMM and LAI anomalies averaged over the eight Brazilian agricultural states listed in Table 2 are shown in Fig. 3 for the period 2003–2013 (upper plots in each panel), along with annual state-level yield estimates from CONAB for corn (1st and 2nd growing seasons), soybean and cotton (lower plots). The dashed lines in the lower plots represent the linear trend for crop yields during the analyzed period. These plots are organized geographically, according to the regions described in Table 2. In this figure, anomalies in 3-month index composites have been further smoothed over a 6-week moving window to suppress noise and more clearly convey co-evolution of yields and indices.

Over these agricultural regions, ESI, TRMM and LAI anomalies show general temporal agreement, capturing major drought and pluvial events (see also the time-series of monthly ESI maps over this period in Fig. 5 of Anderson et al., 2015). A widespread drought afflicted much of central eastern Brazil in 2007. In addition, the northeast experienced an extended drought from 2012 and continuing through 2013 despite heavy rainfall in June, with generally negative impact on detrended yields in PI and BA. The southern region of Brazil has also faced extreme "flash" drought events during 2009 and 2012, causing great losses for the agricultural sector.

Crop yield behavior depicted in Fig. 3 is highly variable between states and years, with some states exhibiting relatively stable yields (e.g., MA) through time and others with strong fluctuations (e.g., PR and RS) – in many cases in synchrony with variations expressed in the remote sensing anomalies, indicating sensitivity to climate drivers. Year-to-year yield fluctuations and trends may also be related to the technological "package" that some states have developed for these
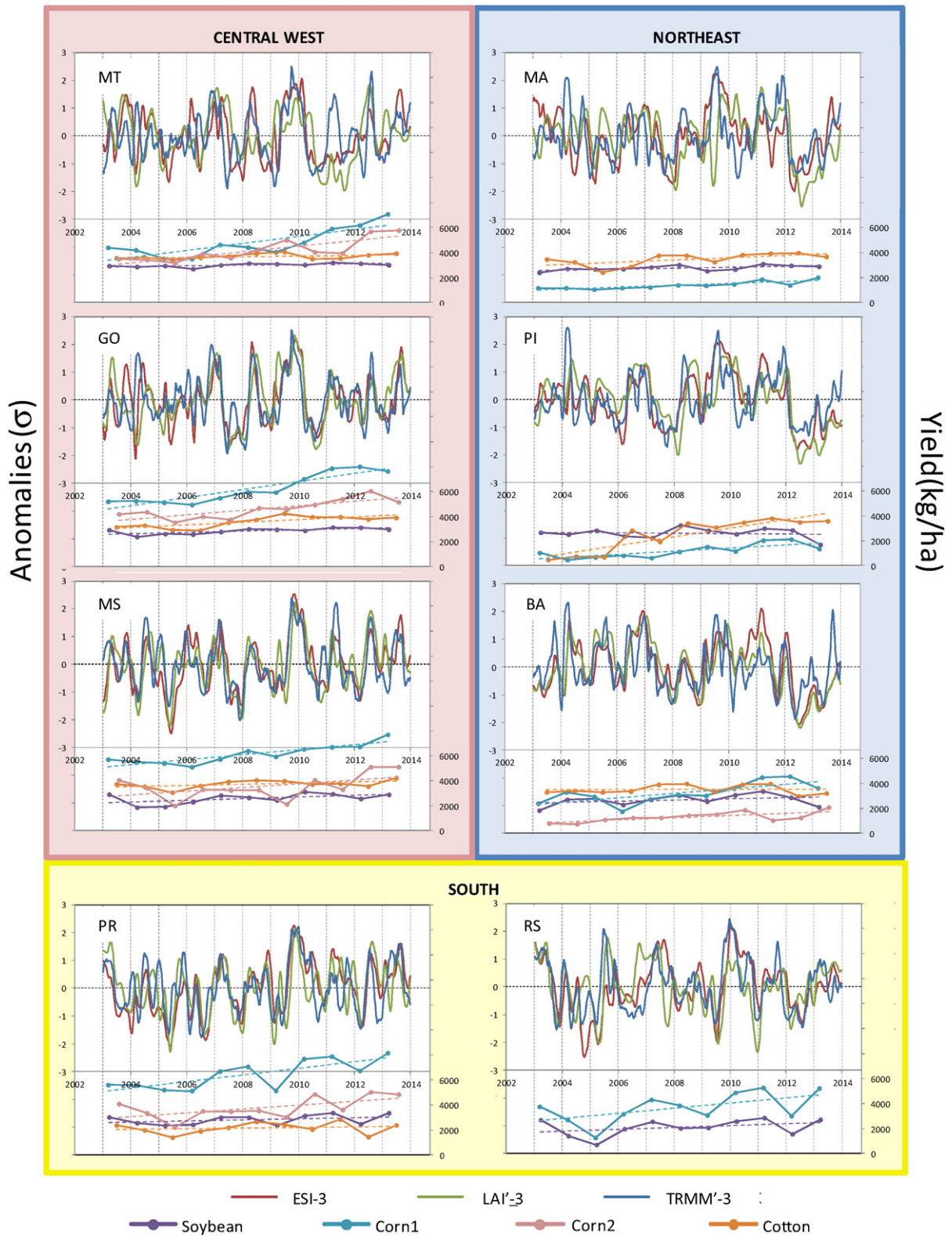
Fig. 3. Annual soybean, cotton and corn yields (two plantings) and trend lines (dashed lines), compared with ESI and anomalies in LAI and TRMM precipitation (3-month composites, smoothed with a 6-week averaging window) for the eight target states.

crops (for example MT, PR and RS). A technological package includes selection of cultivars, tillage practices, sowing and harvesting schedule and technique, fertilizer applications, irrigation, and weed, pest and disease control. Furthermore, market price also plays an important role in the decision making process regarding which crop will be planted and

which technological package will be adopted. These technological and cultural factors may in some places override yield response to weather and soil moisture patterns, and decrease the ability of climatic indicators to accurately predict yield in isolation. In general, this will be more prevalent in the central west, where corporate farms are typically larger and
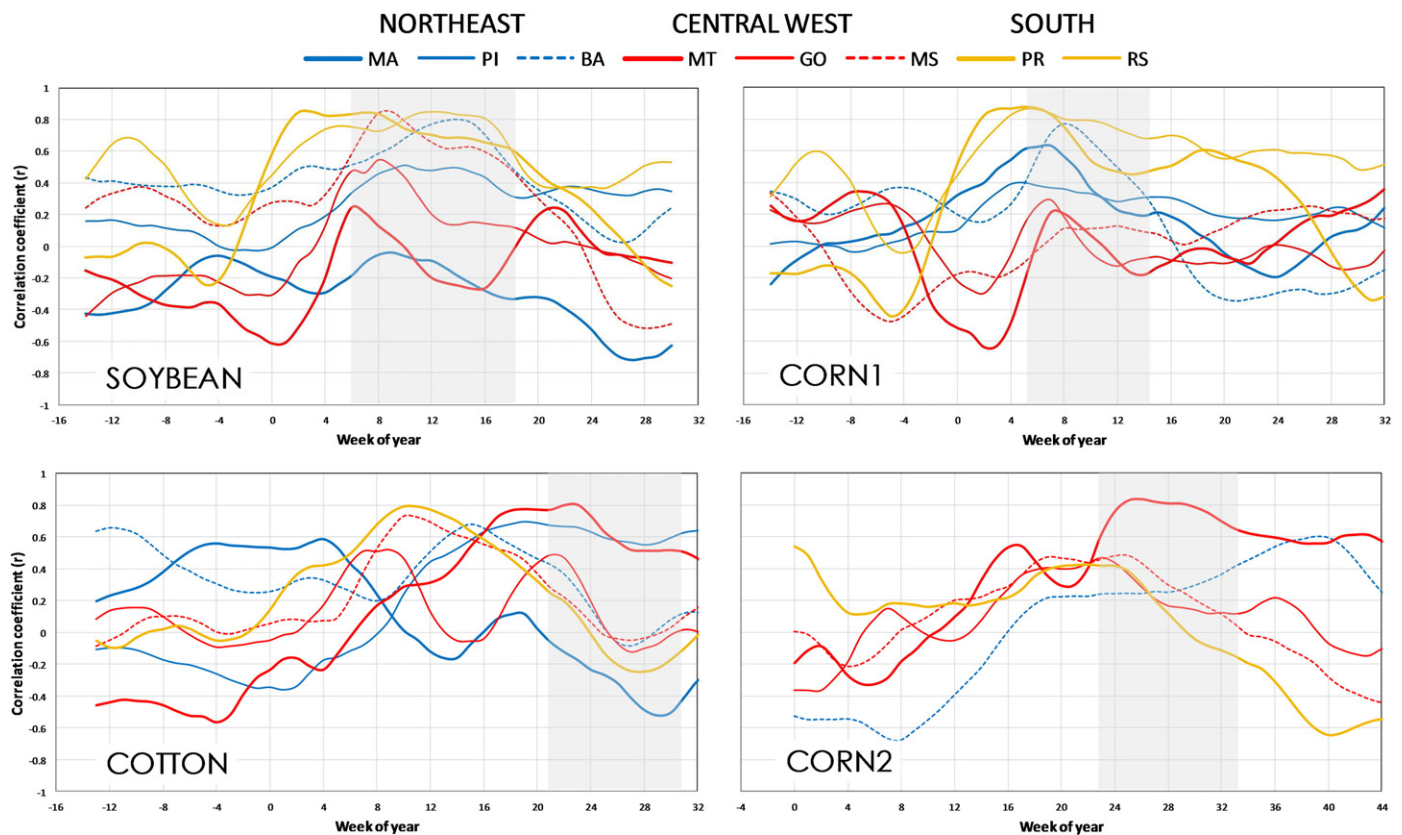
Fig. 4. Correlations between ESI-1 (4-week averaging window) and state-level yield estimates for 2003–2013 as a function of date (week of year) of averaging window end-date, based on 11 samples. Gray shaded area indicates nominal harvest window for each crop.

more highly mechanized. Farms in the northeast and southern states tend to be smaller and more manually operated.

5.1.2. State-level yield correlations with ESI

Fig. 4 shows plots of correlation coefficient (r) computed between state-level yield anomalies and ESI-1 (with additional 4-week averaging for noise suppression) as a function of week of year at the end of the averaging window (see Section 4.2). Approximate windows of harvesting date are also indicated for each crop (soybean: Feb.–Apr.; 1st corn crop: Feb.–Mar.; 2nd corn crop: Jun.–Aug.; cotton: Jun.–Aug.), although harvest can vary widely with region and year. Each correlation consists of 11 points, one for each year during the baseline period 2003–2013; correlations of $|r| > 0.6$ are significant at $p < 0.05$.

5.1.2.1. Soybean.
For soybean, the primary crop in Brazil, yield anomaly correlations with ESI are maximized in a window between January and April, particularly in the southern states of PR and RS, and in BA and MS in the central latitudes – all with peak correlations around 0.8. This coincides with the main flowering and pod-filling stages of soybean growth in Brazil, when yield production is highly sensitive to moisture deficiencies. The states of MT, GO, MA and PI did not exhibit significant correlations with ESI for any week of the year. Yield correlations with LAI and TRMM anomalies were also not statistically significant for these four states (not shown). Looking at Fig. 3, it is evident that detrended yields in MT, GO and MA showed little interannual variability, contributing to the low correlations for these states. For MT and GO, this soybean yield stability is largely due to better climate – with more reliable rainfall during the soybean growing season. The northeastern states of MA and PI had the lowest acreage planted with soybean of all the states considered (Fig. 2), which may also serve to degrade correlations with coarse-scale drought indicators.

Simple correlation analyses with moisture-related indices can be confounded by the fact that low soybean yields can result from both dry and wet conditions. For example soybean yields in MT in 2006 were reduced not due to drought, but due to the increase in the incidence and severity of Asian rust and other problems with pests due to excessive rain and elevated in-canopy wetness duration. The cost of soybean production increased by 600% in 2006 due to intensive fungicide spraying to control rust (Soares, 2007). The following year, a host-free period was introduced in MT to help control future rust outbreaks. Furthermore, the shift toward shorter season cultivars reduces the overlap between the soybean growing season and prominent periods of rust outbreak, lessening damage to yield. Such management changes can lead to a different moisture-yield behavior in subsequent years, further disrupting correlations with satellite-derived moisture indicators such as ESI and TRMM′. In this case additional information will be required to accurately interpret impacts resulting from moisture anomalies, for example from pest or disease models.

Because the strength of correlation depends strongly on the time period of analyses and the degree of yield variability over that period, it is difficult to directly compare the yield correlations reported here with those found in prior studies (e.g., Esquerdo et al., 2011; Liu & Kogan, 2002). For example, Liu and Kogan (2002) correlated AVHRR Vegetation Condition Index and Temperature Condition Index data with CONAB state-level soybean yield anomalies for 1986 to 1995 and obtained different levels of peak correlation. However, the timing of peak sensitivities was similar to those in Fig. 4, with MT, GO and MS peaking during the month of January, when the flowering and grain-filling stages occur, and PR peaking a few weeks earlier and RS a few weeks later.

5.1.2.2. Corn.
Two annual corn plantings are common in many parts of Brazil, with the second season (safrinha) becoming increasingly popular

particularly in MT, MS and GO in recent years due to the release of new hybrids and adoption of new cropping cycles.

For the first planting, corn yields in the southern states of PR and RS have the strongest correlations with ESI, peaking above 0.8 between January and February during the grain-filling stage. In both of these states, the first season corn yields were significantly impacted by the flash droughts in 2009 and 2012, as well as a severe drought event during the 2004/2005 growing season. These severe events serve to increase correlations in the southern states. In addition to the south, correlations in the northeast state of BA approach 0.8, and in MA r peaks around 0.6. Correlations with first corn crop yields in the central west states (MT, GO, MS) as well as PI are not statistically significant over this period of record.

For the second corn growing season, only the states of MT and BA have significant correlation with yields. In this study, the peak correlation for BA is observed very late in the season, driven by specific drought events in 2011 and 2012, which are discussed further in Section 5.1.4. Of the states with high safrinha corn acreage (MT, MS and PR; Table 1), corn crops in MT are most vulnerable to climate variability during critical growth stages. This is because this state experiences higher interannual rainfall variability from May to July, with higher temperatures and water loss through ET, further exacerbating soil moisture conditions when there is a precipitation shortfall. This leads to stronger yield variations and improved correlations with moisture-related indicators.

5.1.2.3. Cotton. Cotton has a longer growing cycle than corn and soybean, and so has a greater potential to be influenced by climatic conditions. Correlations between cotton yields and ESI are statistically significant in the states of PR, MS, BA, MT and PI (Fig. 4). Among these states, timing of the peak correlation is generally related to latitude, with the southern PR and MS states, peaking around week 10, BA around week 15 and the northernmost PI and MT with broad peaks from weeks 16–24. Note that planted cotton acreage in PR dropped to near zero starting in 2006 with a shift in production from the south to the central west (Fig. 2).

5.1.3. Regional yield correlations with ESI, TRMM′ and LAI′

The relative performance of ESI compared to LAI and TRMM anomalies as an early indicator of expected yield was evaluated using the 11-year state-level yield dataset from CONAB. Results from the two-dimensional correlation analyses described in Section 4.2 are shown in Fig. 5, with averaging window end date on the x-axis and length of averaging window on the y-axis. In these analyses, the state-level data were combined regionally to improve statistical sampling and significance. Fig. 5a combines all states and years (All), while panels b–d show regional combinations for the northeast (NE), central west (CW) and southern (S) states, respectively.

The plotting strategy used in Fig. 5 visually summarizes information about relative yield correlation strength (color) for different indices and different regions within Brazil, as well as the relative timing of the peak signal (horizontal position). These plots indicate that in some regions, some degree of additional time-averaging (moving upwards in the plots) helps to improve correlations with yields. For example, Esquerdo et al. (2011) found that a full-season averaging window was optimal for estimating soybean yields in PR using NDVI. However, longer averaging windows are accompanied by a delay in the peak correlation signal – this causes a positive slope in the areas of maximum correlation in Fig. 5. In general, there will be a tradeoff between early notification and confidence in yield forecasts – another argument for looking at multiple agricultural drought indicators.

Overall, the performance of all drought indicators for estimating yields are the highest for Brazilian soybean crops, with ESI yielding the earliest significant correlations several weeks before the harvesting period. Regionally, the southern states collectively show the strongest correlations due in part to several severe drought events that have affected that part of Brazil over the past decade, as noted above. In the northeast, ESI shows the highest correlations with yield for all crops – response to

flash droughts in this region is discussed in Section 5.1.4. The ESI shows superior correlations in the central west states for soybean and cotton, while LAI′ outperforms ESI for the second corn planting and none of the indicators provide useful information regarding yields from the first planting in this region. In this case, other factors are likely limiting yield and yield correlations; for example, cloudiness (impacting solar radiation), high nighttime temperatures, and the dominance of the more profitable soybean production in this area.

The summary plots in Fig. 6 show time series extracted from Fig. 5a (combined region "All") for a 4-week averaging window, identifying windows of maximum index sensitivity for each crop on average over the eight agricultural states targeted in this study and demonstrating reasonable agreement in timing between indices at the national scale. These correlations were computed by combining all state-level yield-index sample pairs, decreasing the threshold of significant correlation at $p < 0.05$ to approximately 0.2 depending on number of years with yield data reported in the CONAB dataset. In general, soybean correlations peak between February and April, the first corn planting between January and February, the second between May and July, and cotton between March and May. In each case, there is a statistically significant correlation several weeks prior to the nominal harvest date. For soybean, cotton and the first corn season, peak correlations are higher for ESI than for LAI anomalies, indicating that value is accrued by combining LST and VI inputs to ALEXI. For these crops, ESI is also better correlated with state-scale yield anomalies than is precipitation. Peak correlations are more similar between all indices for the second corn crop, which may relate to high variability in safrinha crop yields due to less reliable climate conditions in the second season.

5.1.4. Case study: flash droughts in Bahia

To study index responsiveness in more detail, we focus here on the rapid onset drought events that occurred during the safrinha growing season in the state of Bahia in northeast Brazil between 2010 and 2013 (Fig. 7). Most corn production in BA occurs in the western part of the state (part of the fertile "MATOPIBA" agricultural region) during the main cropping season. Safrinha crops are grown primarily in semi-arid northeastern BA, largely for subsistence purposes.

Corn yields in BA for both the 2010/2011 and 2011/2012 growing seasons were elevated for the first crop and depressed in the second crop due to mid-year rainfall deficits (see Fig. 7a). In some regions of BA, farmers did not harvest the second corn crop in 2012 because the yield was too low and it wasn't economically worthwhile. This additional loss of production due to unharvested acreage is not reflected in the CONAB yield data which are reported on harvested area basis. Cotton yields were also negatively impacted in 2011/2012, because the drought that year started earlier and lasted longer than in 2010/2011.

Monthly maps of ESI, LAI′ and TRMM′ showing the evolution of moisture and crop conditions over northeastern Brazil during these two growing seasons are provided in Fig.8. The three indicators capture the cycle of early-season (November to January) moisture availability, aiding the primary corn crop grown in western BA, and mid-year drought in both years in northeastern BA where the bulk of the safrinha corn crops are grown. As indicated in Fig. 7a, ESI indicated a larger amplitude in favorable (positive anomalies, peaking around week 8) and stressed (negative anomalies, week 32–40) conditions during these two years, resulting in higher correlations for ESI with both first and second corn crop yields (Fig. 7b). The oscillating moisture conditions in these two growing seasons led to a strong early season anticorrelation (red tones) with safrinha corn yields in BA and the NE region, particularly for ESI. This anticorrelation feature is to some extent an artifact of the precise sequence of moisture events that occurred in this region over the period of record, but does indicate that this region is highly susceptible to rapid changes in water availability.
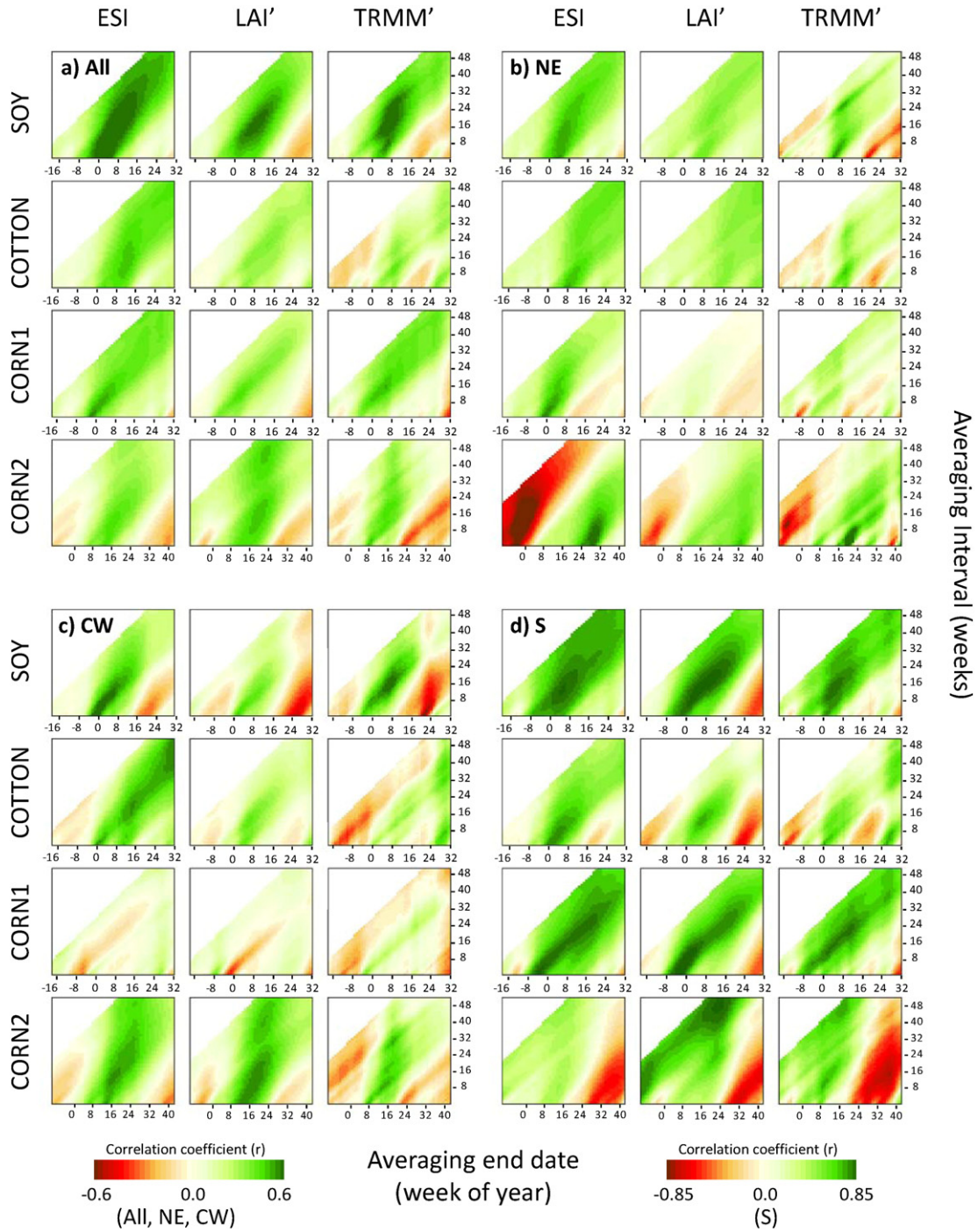
Fig. 5. Correlation of crop yield anomalies with ESI, LAI′ and TRMM′ plotted as a function of index averaging interval and end date for a) all 8 states combined, and the b) northeast (NE), c) central west (CW), and d) southern (S) states. (Note that the plots for S are printed with an expanded color bar due to significantly higher correlations. In addition, the x-axis is shifted to the left for the second corn crop in all regions to capture high correlation periods occurring later in the season.)

5.2. Municipal level yield correlations

To examine regional variability in yield correlation with drought in-dicators in finer spatial detail, we also used yield data reported at the municipality level by IBGE. The spatial resolution of this data set varies across the country, with smaller municipality units in the south and larger units to the north. Yield anomalies for soybean, corn, cotton and wheat were computed for each municipality using Eq. (3) over the pe-riod 2003–2013. Sample maps for 2003–2012 (corn and soybean) are provided in Fig. 9 in comparison with annual ESI patterns for the

January–February–March (JFM) composite interval – a period of peak sensitivity identified in Figs. 4–6 for soybean and the first corn planting. In general, there is good spatial correspondence between ESI and yield anomalies in corn and soybean, particularly in the southern states. Sim-ilar spatiotemporal patterns were evident in the cotton and wheat yield anomalies (not shown), although the spatial coverage for these two crops is not as extensive as for corn and soybean.

Less correspondence is observed between the drought indicators and corn yield anomalies in the northeast. This is due in part to the fact that IBGE does not distinguish between cropping cycles – optimal
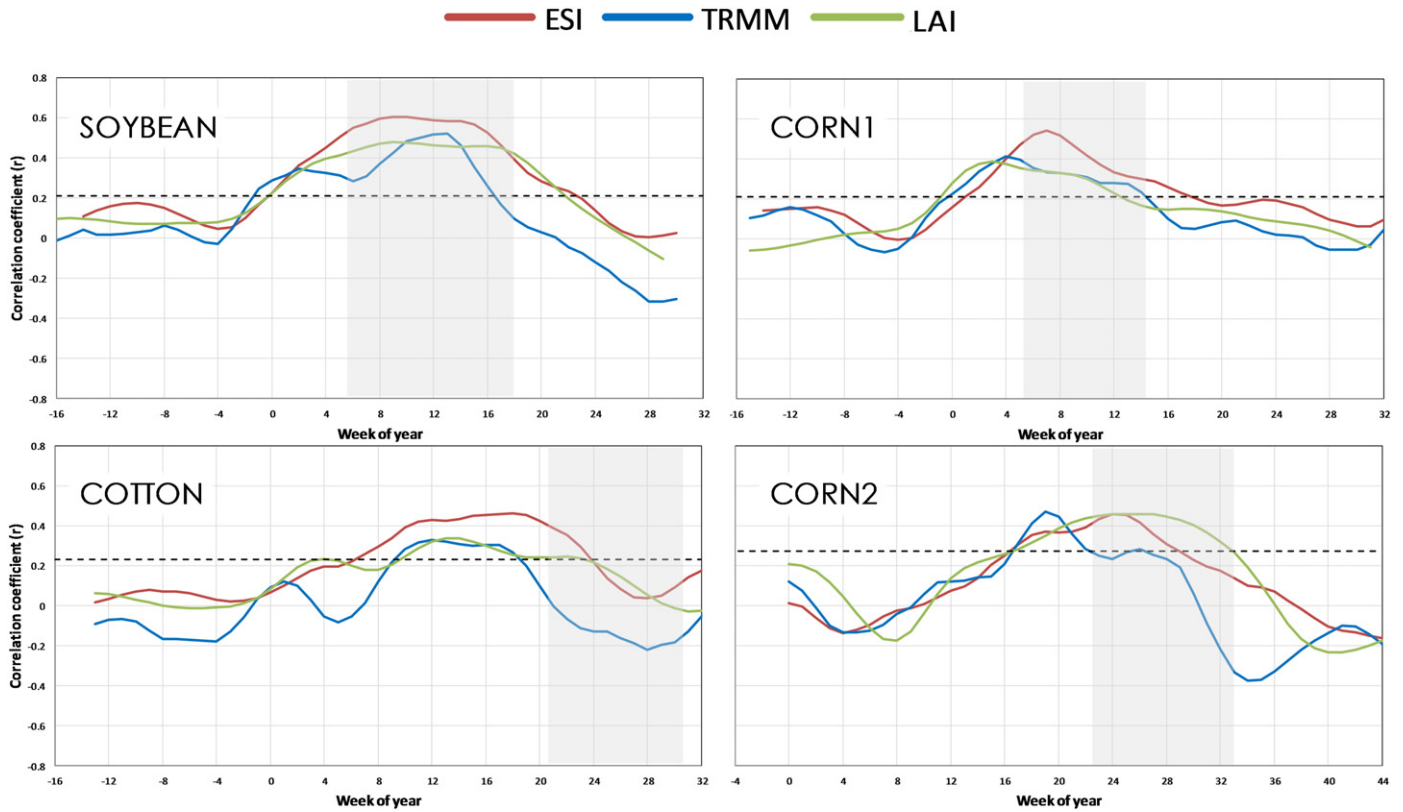
Fig. 6. Correlations between 1-month ESI composites, TRMM precipitation anomalies and MODIS LAI anomalies and state-level yield estimates for 2003–2013 as a function of date (week of year) of composite end-date. Correlations are computed for all states combined. Gray shaded indicates nominal harvest date for each crop, while horizontal line indicates level of significant correlation at p < 0.05 (n is variable, depending on number of years of yield data available in CONAB dataset).

correlations with the safrinha corn crop occur later in the season. The rapid cycling of seasonal drought conditions in northeast Brazil during 2011–2012 described in Section 5.1.4 led to spatial disparities in corn production over the state of BA particularly in 2011, with higher than average yields in the western MAPITOBA region from the first corn crop (consistent with the JFM ESI map in Fig. 9), and depressed yields in eastern BA associated with the failure of safrinha corn crops (more consistent with the July and August 2011 ESI maps in Fig. 8). Again, yield reductions due to unharvested (abandoned) acreage during the second corn season are not incorporated into the IBGE estimates, so crop losses in eastern BA are somewhat underrepresented in Fig. 9. In 2012, many of these municipalities did not report yields where crops were abandoned (appearing blank in Fig. 9).

To quantify spatiotemporal variability in yield correlations at the municipality level, a time series of IBGE yield-index correlation maps was computed at 7-day intervals over the Brazilian growing season for each drought indicator, using 3-month composites (ESI-3, TRMM′-3 and LAI′-3). Example maps are shown in Fig. 10, sampled at times of peak regional sensitivity to corn and soybean yields as identified in the state-level analyses. Also shown are maps of coefficient of variation in soybean and corn yields, as well as in f_{RET}, TRMM precipitation and MODIS LAI over the period of record. Areas of strong annual yield and index variability (high CV) are spatially collocated, primarily in the southern and northeastern states. This is advantageous, indicating the indices have sensitivity in regions where yield is highly variable from year to year. These are also areas where yield-index correlations are the highest, which is reasonable given that the magnitude of Pearson's r can be strongly affected by the degree of variability inherent in the datasets being correlated. As indicated in the state-level analyses, peak index-yield correlation strength varies regionally and with cropping cycle. While the IBGE yield database does not distinguish between first and second corn harvests, the correlations for corn in Fig. 10 peak

later in the season in states where the second crop is more prevalent, such as MT and MS in the central west and in the northeast.

Fig. 11 shows the date and strength of peak index correlation with IBGE soybean and corn yields, summarized for the eight target agricultural states in Table 1. These state-level aggregates were computed by averaging municipality-level values weighted by crop production from 2009 (mid-point in study; see maps in Fig. 10), thereby focusing primarily on response in the highest productivity regions. A marked north-south gradient in peak correlation in all indicators is evident for soybean yields with the strongest correlations in the southern states, confirming trends identified with the state-level CONAB datasets (Fig. 4). For soybean, peak correlations are marginally stronger with ESI in most states (r = 0.62 on average), with LAI anomalies yielding the lowest correlations (r = 0.50), especially in the northeast. Date of peak predictive signal is relatively uniform across the country, with ESI providing earlier indication of soybean yield impacts by 10 days on average in comparison with TRMM′ and 25 days in comparison with LAI′. In the northeastern states, ESI peak correlations occur 20–60 days earlier than TRMM′ or LAI′.

Date of peak signal is more variable regionally for corn crops, likely relating to the multiplicity in cropping cycles. In the central western states of MS and MT where the majority of corn crop acres planted occurs in the second season (Fig. 2, Table 2), peak correlations occur around DOY 160, consistent with the peaks between week 20 and 24 (DOY 140-170) associated with CONAB state data for the second corn crop in Fig. 6. In the other states, peak correlations occurred around DOY 80-120, similar to patterns for the first corn crop in Fig. 6. In relation to IBGE corn yields (first and second crops combined), precipitation anomalies yielded marginally higher peak signal in most states, with the exception of BA. As discussed in Section 5.1.4, the ESI was better able to reproduce the rapid intra-annual cycling in crop conditions experienced in BA in 2011–2013.
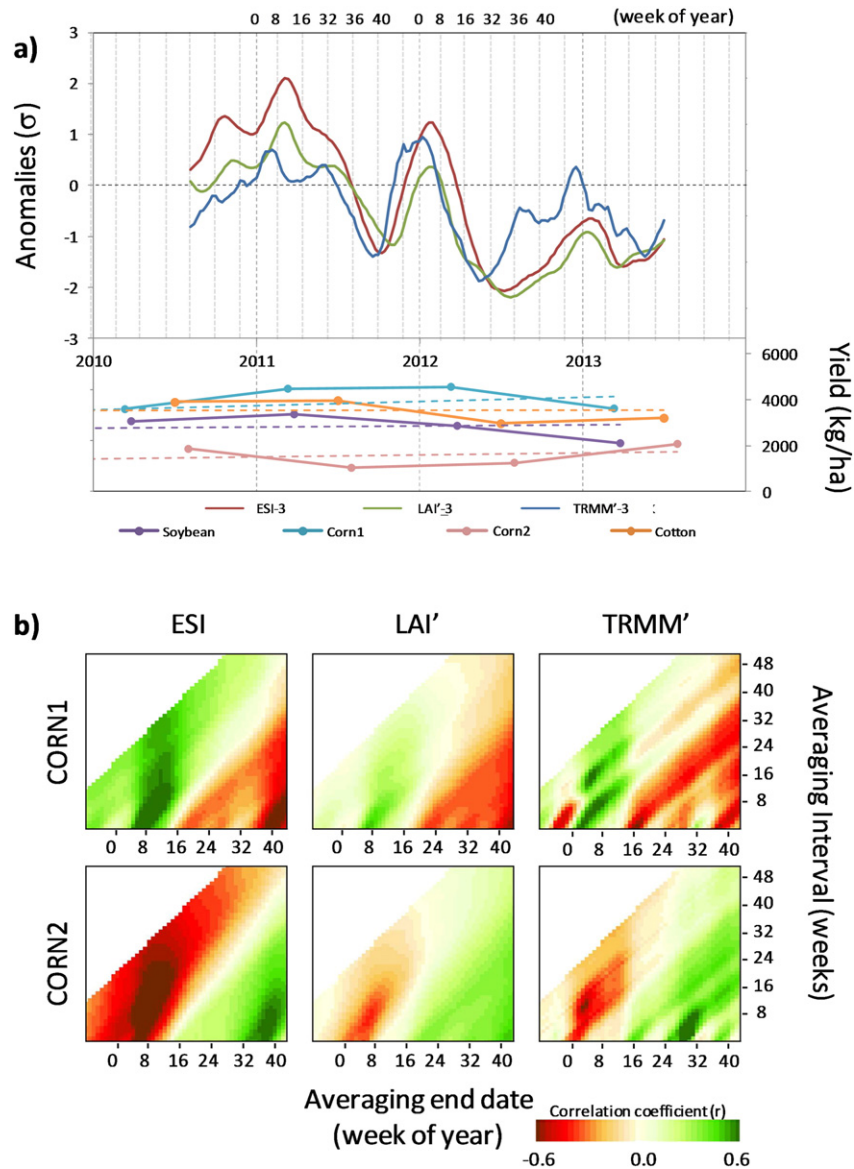
Fig. 7. Yield and index relationships over BA during the 2010/2011 and 2011/2012 growing seasons: a) similar to Fig. 3, but focused on 2010–2013; b) similar to Fig. 5, but isolating BA state from NE region.

6. Discussion

6.1. ESI utility in monitoring agricultural drought

In comparing the relative performance of ET, precipitation and LAI anomaly indices, assessed here using yield anomaly correlations, the ESI appears to have some advantage in terms of timing and strength of correlative signal, particularly for soybean, cotton, and primary corn crop. Correlations at the state level were similar between indices for the safrinha corn crop, and precipitation deficits were marginally more successful in explaining annual yield variability for the two corn crops combined as reported at the municipality level. An exception was noted in the state of Bahia in northeast Brazil, where ESI responded quickly to rapid intra-annual cycling of wet and dry conditions during the 2011–2012 growing seasons, providing better correlation with first and second corn crop yield anomalies. LAI correlations were lower for all crops examined, and the peak signal occurred later in the season. Indices relating to plant green biomass are considered to be slow-response variables, lagging surface/canopy temperature which responds more rapidly in response to crop stress (Moran, 2003).

Despite limitations of individual indicators, concomittant development of negative ET, vegetation index, and precipitation anomalies over timescales of several weeks provides valuable corroborative evidence of impending yield impacts. A robust suite of complementary remotely sensed crop health and moisture indicators will benefit climate vulnerability assessments and development of national drought preparedness plans, as currently underway in northeastern Brazil (Gutiérrez et al., 2014). One outcome of this plan includes the recent development of a regional Drought Monitor (monitordesecas.ana.gov.br) for northeast Brazil, modeled after the U.S. Drought Monitor (USDM; Svoboda et al., 2002) approach which integrates drought information from multiple sources and indicators, and includes consideration of reported drought impacts. ESI has been demonstrated to agree well with drought severity classifications recorded in the USDM archive (2013; Anderson et al., 2011), and to lead USDM and other VI- and precipitation-based indicators during development of rapid onset, or "flash" drought events (Otkin et al., 2013, 2014). Similar analyses are underway in comparison with monthly archived assessments from the Northeast Brazil Drought Monitor.
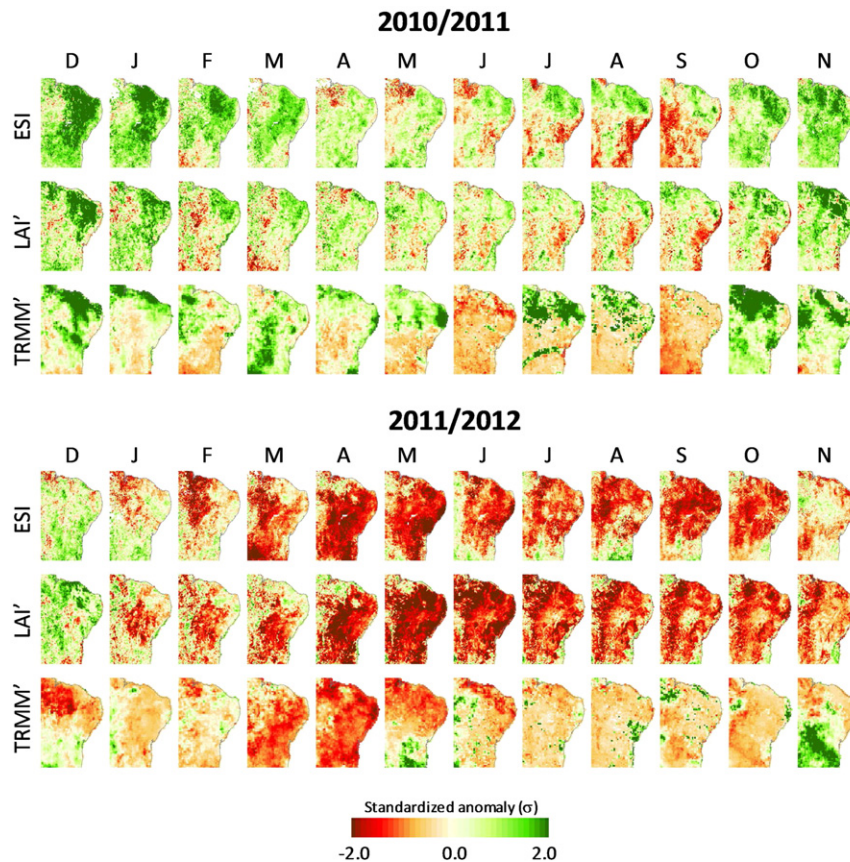
Fig. 8. Comparison of ESI, LAI′ and TRMM′ (1-month composites) over the 2010/2011 and 2011/2012 growing seasons in northeastern Brazil showing development of mid-season drought.

6.2. Water limitations on crop growth — ESI utility in yield gap analyses

Yield-satellite index correlation analyses at both the state and municipal levels identified agricultural regions within Brazil where crop yields have been climatically sensitive to moisture deficits during the past decade, primarily in the southern and northeastern states. These results corroborate the findings of Sentelhas et al. (2015) who used agrometeorological modeling to analyze soybean yield gaps over Brazil. Using crop models for attainable and potential yield forced at discrete points by surface weather station data along with actual yield information from IBGE and CONAB for 1980 to 2011, they determined that the soybean yield gap in Brazil due to water limitations was the highest in the southern states of RS, PR, MS as well as Sao Paulo (northeastern states were not included in that study) due to recurrent severe droughts. Here we find that during the period 2003–2013, strong variability in the remote sensing indicators studied coincided with regions of large interannual crop yield variability in Brazil (Fig. 10).

This suggests that at the global scale, remote sensing – particularly of moisture variables like ET and rainfall – can play an important role in identifying climatically sensitive agricultural systems, providing a diagnostic assessment of areas where there may be a strong water limitation component in the yield gaps. Large-scale efforts, such as the Global Yield Gap and Water Productivity Altas (www.yieldgap.org) will benefit by integrating geospatial information from satellites to provide better spatial and temporal coverage (Lobell, 2013). Diagnostic information about moisture variability from the long-term ESI record may help to refine the climatic zonations used to upscale field-scale gap simulations to larger regions (van Bussel et al., 2015).

We note that sensitivity of the ET and precipitation indices to crop yield variability was not isolated to areas in Brazil that are classically defined as "water-limited" under the Budyko (Budyko, 1974) aridity index

definition. While the climate in northeast Brazil is classified as semi-arid and crop growth is normally water-limited, southern Brazil is classified humid but is still subject to periodic extreme drought events (Alvares, Stape, Sentelhas, Goncalves, & Sparovek, 2014). In this study drought index-yield correlations tended to be high in water-limited regions, as was also demonstrated by López-Lozano et al. (2015) over Europe. In Brazil, there is also sensitivity in the southern states, which are identified as "equitant" by McVicar, Roderick, Donohue, and Van Niel (2012), straddling the boundaries between water and energy limitations.

6.3. Utility in yield forecasting and crop modeling

Several factors confound simple interpretation of remotely sensed moisture indicators such as ESI in terms of yield impacts. While drought during physiologically sensitive times in the crop growth cycle will clearly reduce yield, crop failures can also accompany pluvial periods, leading to waterlogging and favoring pest and disease occurrences such as Asian soybean rust, white mold and mildew that benefit from warm and moist conditions. Thus moisture conditions at both extremes can lead to yield reductions. Sentelhas et al. (2015) note that Brazilian crop yields can vary significantly even given similar levels of ET (moisture availability) due to differences in management, soil properties (e.g., organic matter content), sowing date and cultivar. A more robust interpretation of remote sensing data as leading indicators of yield requires integration with crop, pest and disease models that will properly consider moisture and temperature extremes occuring during critical phenological stages of the crop growth cycle, as well as evolution in plant light harvesting capabilities (sunshine and green leaf area).

Models of varying complexity have been developed to forecast yields, including index regression models of the type explored here, simple agrometeorological models that consider sensitivity to moisture,
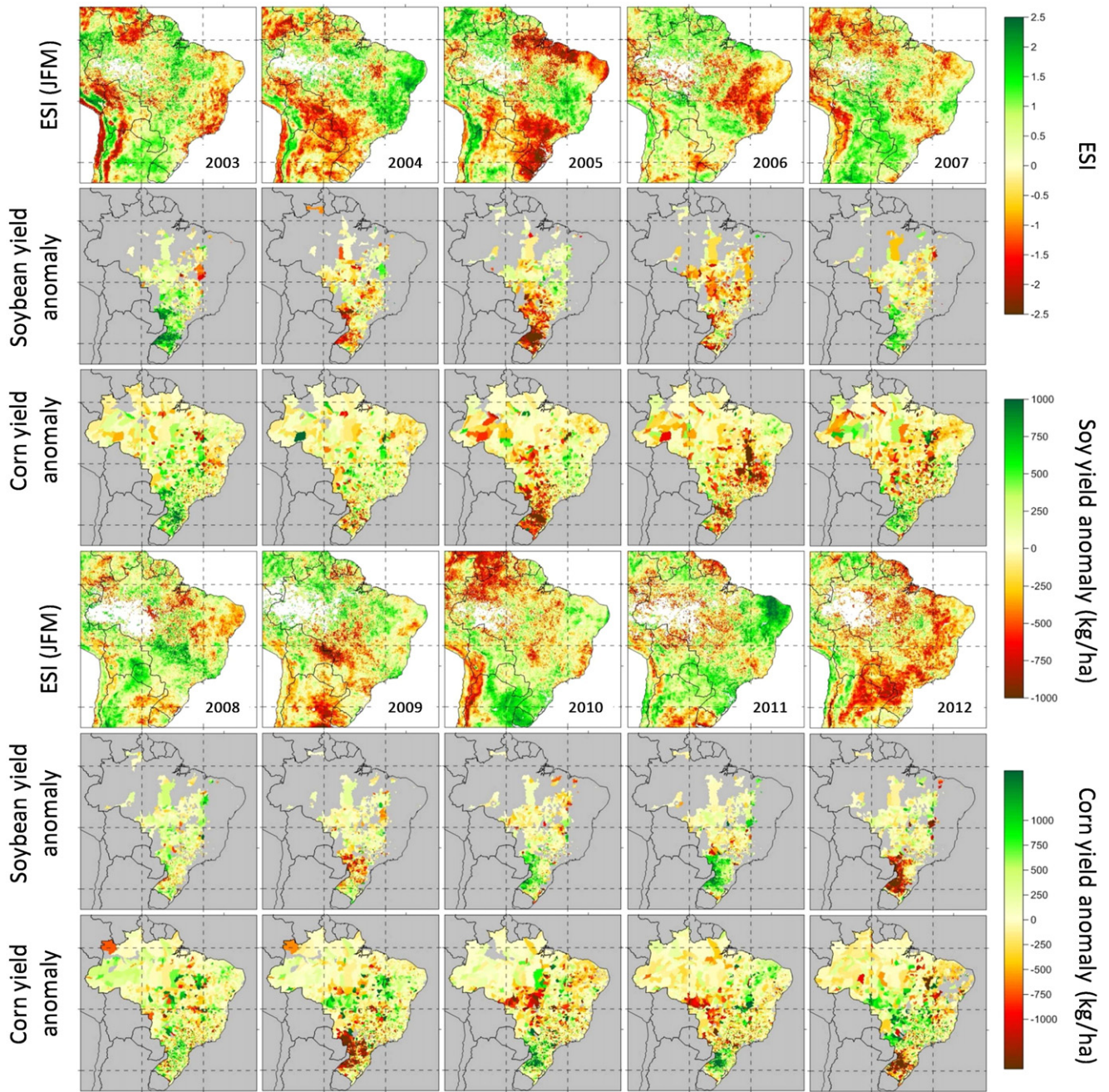
Fig. 9. Annual JFM ESI maps, with annual anomalies in municipal level corn and soybean yields reported by IBGE for 2003–2012.

temperature and light limitations, and crop simulations that represent plant biophysical relationships in more physical detail (see review by Basso et al. (2013)). Efforts to integrate remote sensing into agrometeorological models for Brazil have initially focused on NDVI as a proxy for biomass or leaf area, diagnostically capturing management impacts on crop development that are difficult to model a priori with fine spatial detail (Fontana, Melo, Klering, Berlato, & Ducati, 2006). Moisture limitations can be incorporated using estimates of the relative ET ratio (f_{RET}) (e.g., Doorenbos & Kassam, 1979; Jensen, 1968; Rao, Sarma, & Chander, 1988) derived from a simplified soil water balance approach using weather and soil texture data (e.g., Rudorff & Batista, 1990), or from remote sensing (Teixeira et al., 2013).

Mishra et al. (2013) demonstrated use of f_{RET} from ALEXI ESI to update soil moisture status in a gridded application of the Decision Support System for Agrotechnology Transfer (DSSAT) crop simulation model over rainfed and irrigated corn in southeastern U.S., and found

it served as a reasonable proxy for in-situ measurements of rainfall. An alternate version of the two-source land-surface representation in ALEXI uses an analytical light-use efficiency approach for estimating canopy resistance and coupled carbon, energy and water fluxes (Anderson, Norman, Meyers, & Diak, 2000), leveraging stress signals diagnosed from the thermal retrieval of canopy temperature (Anderson et al., 2008; Houborg, Anderson, Daughtry, Kustas, & Rodell, 2011; Schull, Anderson, Houborg, Gitelson, & Kustas, 2015). Accumulated carbon flux from this framework, responding to both light and moisture limitations, may further improve remotely sensed yield estimation capabilities.

6.4. Issues of spatial resolution

The 0.1 deg. spatial resolution of the ET and LAI remote sensing products used in this study has undoubtedly degraded reported correlations
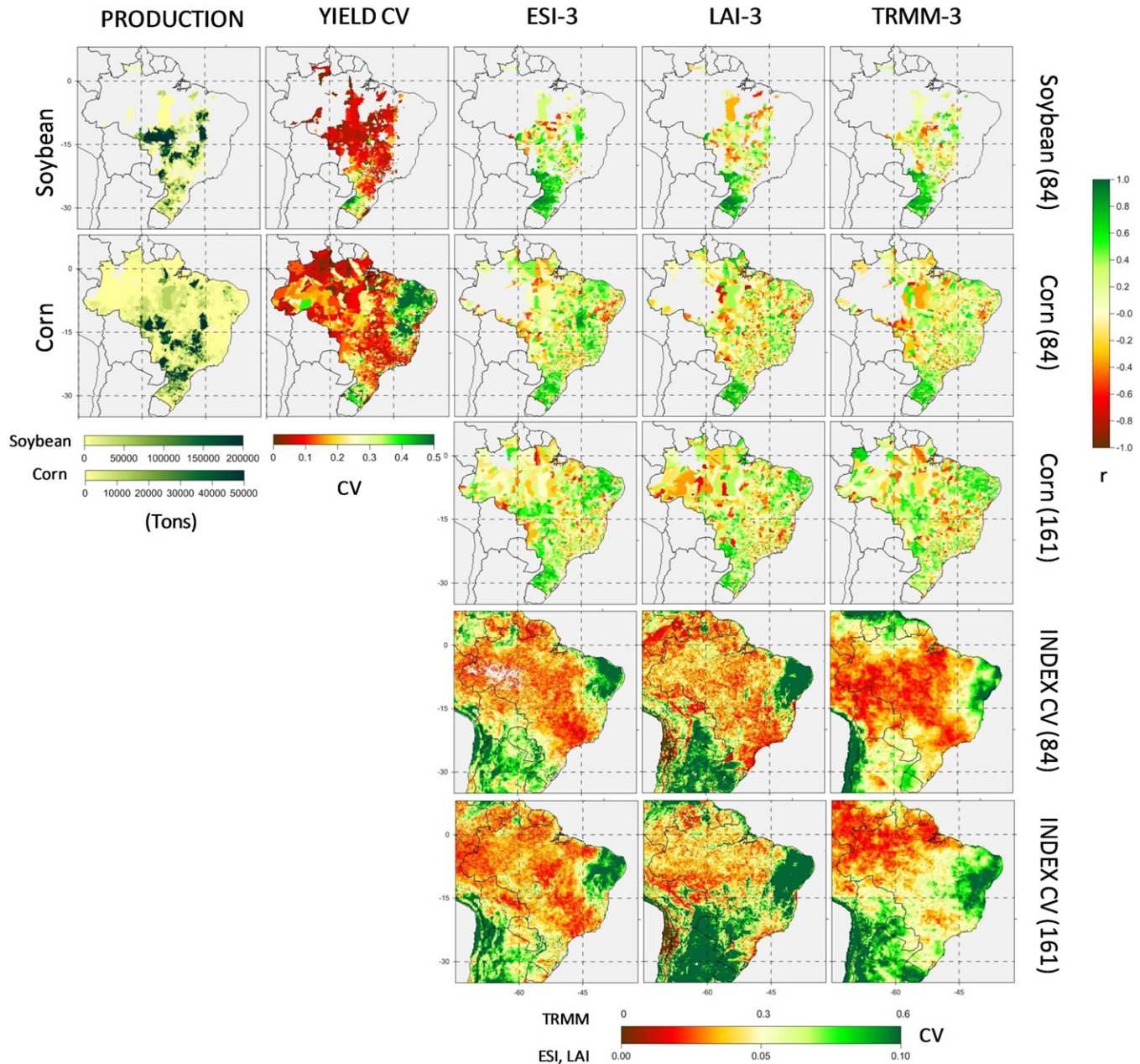
Fig. 10. Production for 2009 (first column) and coefficient of variation (CV; second column) in municipal level corn and soybean yield estimates (IBGE); (bottom row) CV in f_RET, LAI and TRMM precipitation (3-month composites ending DOY 84 and 161); (rest) correlation between yield and index anomalies (3-month composites ending on DOY 84 and 161) over the period 2003–2013 (n = 11).

with crop yields, as most pixels at this coarse scale will carry composite surface moisture and biomass signals associated with a mixture of sub-pixel crop types at different stages of development. At present, only the Landsat series of satellites provides routine measurements in both TIR and reflective bands capable of resolving individual farm fields of typical size. At the Landsat scale (30 m in both band classes, using thermal sharpening techniques; Gao, Kustas, & Anderson, 2012), water use and phenology can be differentiated by crop type and land management practice (Anderson, Allen, Morse, & Kustas, 2012), making this an optimal scale for assessments of yield and water productivity (Lobell, 2013; Lobell, Thau, Seifert, Engle, & Little, 2015). Data fusion methodologies, combining the high spatial resolution of Landsat with the daily temporal frequency of MODIS or similar moderate resolution systems, facilitate estimation of daily ET and vegetation indices at sub-field scales (Cammalleri, Anderson, Gao, Hain, & Kustas, 2013; Cammalleri, Anderson, Gao, Hain, & Kustas, 2014; Semmens et al., in press). At

these scales, ESI time series in combination with remotely sensed phenology could be used to empirically investigate and improve parameterization of moisture stress functions and alarms implemented in crop simulation models and operational yield estimates (Gao et al., 2015). High resolution seasonal ET accumulated in pure (unmixed) 30-m pixels can be ratioed with reported yield data to assess water productivity differentiated by crop type at the municipal or state level.

7. Conclusion

A suite of satellite-based indicators describing anomalies in precipitation (from TRMM), LAI (from MODIS), and the relative ET ratio (i.e., ESI) were correlated with yield data for three major Brazilian crops (soybean, corn and cotton) reported at state and municipality levels over the period 2003–2013. In general the indicators provided similar spatial patterns in correlation strength, with the highest
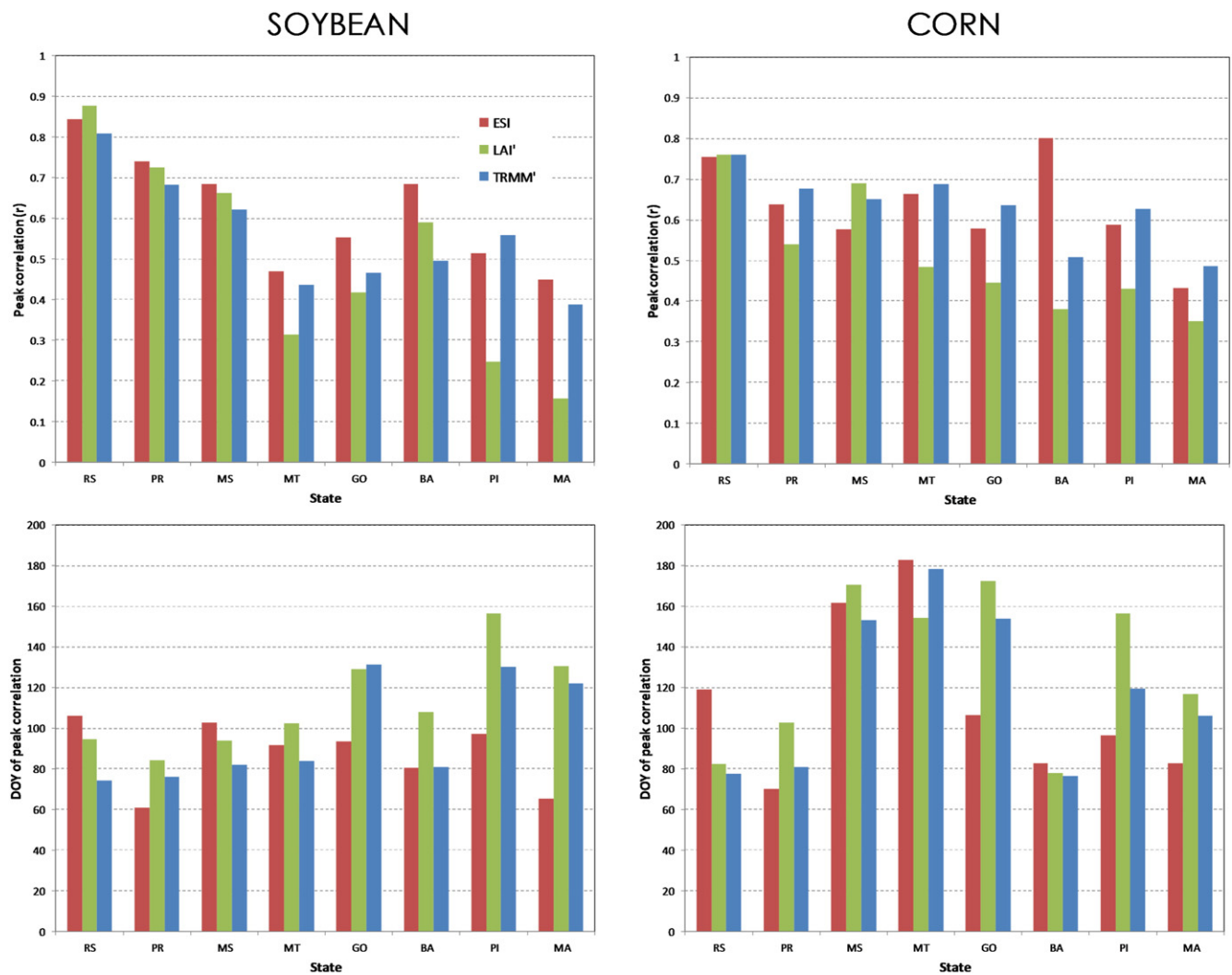
Fig. 11. Date and strength of peak correlation of ESI, LAI′ and TRMM′ indicators with IBGE soybean and corn anomalies for the 8 target agricultural states.

correlations occurring in regions with the highest index and yield variability over the period of record – due in part to flash drought events that have occurred in the northeast and southern states of Brazil during the past decade.

Timing of peak index correlation with at-harvest yields varied by crop and region, and typically occurred during critical growth stages (flowering and grainfilling). At regional scales using state-level yield data from CONAB, the ESI provided higher correlations for most crops and regions in comparison with TRMM and LAI anomalies. Using finer scale yield data at the municipality level from IBGE, ESI showed higher and substantially earlier peak correlations with soybean yields by 10 to 25 days in comparison with TRMM and LAI, respectively. In most states, TRMM peak correlations were marginally higher with IBGE corn yields. A notable exception was the state of Bahia in northeast Brazil, where ESI was better able to capture rapidly developing late-season droughts that differently impacted the first and second corn crops in 2011 and 2012. The difference in performance between ESI and LAI anomalies indicates utility for drought monitoring in combining LAI and LST indicators within a physically based model of crop water use.

Because negative yield anomalies can accompany both dry and moist conditions in Brazil, resulting from droughts, floods and moisture-loving pests or diseases, simple regression-based yield forecasts using moisture-related satellite indices can be confounded in some regions. A more robust approach to yield estimation would involve integration with crop modeling systems accounting for likelihood of pest and disease outbreak. The regression analyses presented here provide insight into when and where different indicators are likely to add significant value to yield forecasts.

References

Allen, R. G., Pereira, L. S., Raes, D., & Smith, M. (1998). *Crop evapotranspiration: guidelines for computing crop water requirements, United Nations FAO, Irrigation and Drainage Paper 56.* Italy: Rome, 300 (In).

Alvares, C. A., Stape, J. L., Sentelhas, P. C., Goncalves, J., & Sparovek, G. (2014). Köppen's climate classification map for Brazil. *Meteorologische Zeitschrift, 22*, 711–728.

Anderson, M. C., Hain, C. R., Wardlow, B., Mecikalski, J. R., & Kustas, W. P. (2011). Evaluation of drought indices based on thermal remote sensing of evapotranspiration over the continental U.S. *Journal of Climate, 24*, 2025–2044.

Anderson, M. C., Norman, J. M., Kustas, W. P., Houborg, R., Starks, P. J., & Agam, N. (2008). A thermal-based remote sensing technique for routine mapping of land-surface carbon, water and energy fluxes from field to regional scales. *Remote Sensing of Environment, 112*, 4227–4241.

Anderson, M. C., Norman, J. M., Mecikalski, J. R., Otkin, J. A., & Kustas, W. P. (2007a). A climatological study of evapotranspiration and moisture stress across the continental U. S. based on thermal remote sensing: I. Model formulation. *Journal of Geophysical Research, 112*, D10117. http://dx.doi.org/10.1029/2006JD007506.

Anderson, M. C., Norman, J. M., Mecikalski, J. R., Otkin, J. A., & Kustas, W. P. (2007b). A climatological study of evapotranspiration and moisture stress across the continental U. S. based on thermal remote sensing: II. Surface moisture climatology. *Journal of Geophysical Research, 112*, D11112 (doi:11110.11029/12006JD007507).

Anderson, M. C., Norman, J. M., Meyers, T. P., & Diak, G. R. (2000). An analytical model for estimating canopy transpiration and carbon assimilation fluxes based on canopy light-use efficiency. *Agricultural and Forest Meteorology, 101*, 265–289.

Anderson, M. C., Zolin, C., Hain, C. R., Semmens, K. A., Yilmaz, M. T., & Gao, F. (2015). Comparison of satellite-derived LAI and precipitation anomalies over Brazil with a thermal infrared-based Evaporative Stress Index for 2003–2013. *Journal of Hydrology*. http://dx.doi.org/10.1016/j.jhydrol.2015.1001.1005.

Anderson, M. C., Allen, R. G., Morse, A., & Kustas, W. P. (2012). Use of Landsat thermal imagery in monitoring evapotranspiration and managing water resources. *Remote Sensing of Environment, 122*, 50–65.

Anderson, M. C., Hain, C. R., Otkin, J. A., Zhan, X., Mo, K. C., Svoboda, M., ... Pimstein, A. (2013). An intercomparison of drought indicators based on thermal remote sensing and NLDAS-2 simulations with U.S. Drought Monitor classifications. *Journal of Hydrometeorology, 14*, 1035–1056.

Basso, B., Cammarano, D., & Carfagna, E. (2013). Review of crop yield forecasting methods and early warning systems. *GS SAC – Improving methods for crops estimates.* Rome, Italy: FAO Publication.

Bastiaanssen, W. G. M., & Ali, S. (2003). A new crop yield forecasting model based on satellite measurements applied across the Indus Basin, Pakistan. *Agriculture, Ecosystems and Environment, 94*, 321–340.

Becker-Reshef, I., Vermote, E., Lindeman, M., & Justice, C. O. (2010). A generalized regression-based model for forecasting winter wheat yields in Kansas and Ukraine using MODIS data. *Remote Sensing of Environment, 114*, 1312–1323.

Bolten, J. D., Crow, W. T., Zhan, X., Jackson, T. J., & Reynolds, C. A. (2010). Evaluating the utility of remotely sensed soil moisture retrievals for operational agricultural drought monitoring. *IEEE Journal of Selected Topics in Applied Earth Observations and Remote Sensing, 3*, 57–66.

Brown, M. E. (Ed.). (2008). *Famine early warning systems and remote sensing data.* Berlin: Springer-Verlag.

Budyko, M. I. (1974). *Climate and life.* New York: Academic Press.

van Bussel, L. G. J., Grassini, P., Van Wart, J., Wolf, J., Claessens, L., Yang, H., ... van Ittersum, M. K. (2015). From field to atlas: Upscaling of location-specific yield gap estimates. *Field Crops Research, 177*, 98–108.

Cammalleri, C., Anderson, M. C., Gao, F., Hain, C. R., & Kustas, W. P. (2013). A data fusion approach for mapping daily evapotranspiration at field scale. *Water Resources Research, 49*, 1–15. http://dx.doi.org/10.1002/wrcr.20349.

Cammalleri, C., Anderson, M. C., Gao, F., Hain, C. R., & Kustas, W. P. (2014). Mapping daily evapotranspiration at field scales over rainfed and irrigated agricultural areas using remote sensing data fusion. *Agricultural and Forest Meteorology, 186*, 1–11.

Delgado, P. R., & Zanchet, M. S. (2011). *A importância da expansão da área de lavoura para o aumento da produção agrícola no Paraná.* Instituto Paranaense de Desenvolvimento Econômico e Social (EPARDES), 1–12 (In).

Doorenbos, J., & Kassam, A. H. (1979). Yield response to water. *FAO Irrigation and drainage paper, No 33.* Rome: FAO.

Doraiswamy, P. C., Akhmedov, B., Beard, L., Stern, A., & Mueller, R. (2007). *Operational prediction of crop yields using MODIS data and products.* Workshop proceedings: Remote sensing support to crop yield forecast and area estimates, ISPRS Archives XXXVI-8/W48.

Doraiswamy, P. C., Sinclair, T. R., Hollinger, S., Akhmedov, B., Stern, A., & Prueger, J. (2005). Application of MODIS derived parameters for regional crop yield assessment. *Remote Sensing of Environment, 97*, 192–202.

Esquerdo, J. C. D. M., Júnior, J. Z., & Antunes, J. F. G. (2011). Use of NDVI/AVHRR time-series profiles for soybean crop monitoring in Brazil. *International Journal of Remote Sensing, 32*, 3711–3727.

FAO (2003). *World agriculture towards 2015/2030: an FAO perspective.* , 432 (Rome).

Fernandes, J. L., Rocha, J. V., & Lamparelli, R. (2011). Sugarcane yield estimates using time series analysis of spot vegetation images. *Science in Agriculture, 68*, 139–146.

Foley, J. A., Ramankutty, N., Brauman, K. A., Cassidy, E. S., Gerber, J. S., Johnston, M., ... Zaks, D. P. M. (2011). Solutions for a cultivated planet. *Nature, 478*, 337–342.

Fontana, D. C., Melo, R. W., Klering, E. V., Berlato, M. A., & Ducati, J. (2006). Uso de modelos agrometeorológicos na estimativa do rendimento de lavouras, Instituto Brasileiro de Geografia e Estatística. *Documento apresentado para discussão no II Encontro Nacional de Produtores e Usuários de Informações Sociais, Econômicas e Territoriais* (9 pp.).

Gao, F., Hilker, T., Zhu, X., Anderson, M. C., Masek, J., Wang, P., & Yang, Y. (2015). *Fusing Landsat and MODIS data for vegetation monitoring, 3.* (pp. 47–60). IEEE Geoscience and Remote Sensing Magazine.

Gao, F., Kustas, W. P., & Anderson, M. C. (2012). A data mining approach for sharpening thermal satellite imagery over land. *Remote Sensing, 4*, 3287–3319.

Gao, F., Morisette, J. T., Wolfe, R. E., Ederer, G., Pedelty, J., Masuoka, E., ... Nightingale, J. (2008). An algorithm to produce temporally and spatially continuous MODIS LAI time series. *IEEE Geoscience and Remote Sensing Letters, 5*(1), 60–64.

Global Harvest Initiative (2014). *2014 Global agricultural productivity report.*

Guan, K., Berry, J., Zhang, Y., Guanter, L., Badgley, G., & Lobell, D. B. (2015). Improving the monitoring of crop productivity using spaceborne solar-induced fluorescence. *Global Change Biology.* http://dx.doi.org/10.1111/gcb.13136 (in press).

Gusso, A., Ducati, J., Veronez, M. R., Sommer, V., & da Silveira, L. G., Jr. (2014). Monitoring heat waves and their impacts on summer crop development in southern Brazil. *Agricultural Sciences, 5*, 353–364.

Gusso, A., Ducati, J. R., Veronez, M. R., Arvor, D., & da Silveira, L. G., Jr. (2013). Spectral model for soybean yield estimate using MODIS/EVI data. *International Journal of Geosciences, 4*, 1233–1241.

Gutiérrez, A. P. A., Engle, N. L., De Nys, E., Molejón, C., & Martins, E. (2014). Drought preparedness in Brazil. *Weather and Climate Extremes.* http://dx.doi.org/10.1016/j.wace. 2013.1012.1001i.

Holmes, T., Crow, W. T., Hain, C. R., Anderson, M. C., & Kustas, W. P. (2014). Diurnal temperature cycle as observed by thermal infrared and microwave radiometers. *Remote Sensing of Environment, 158*, 110–125.

Houborg, R., Anderson, M. C., Daughtry, C. S. T., Kustas, W. P., & Rodell, M. (2011). Using leaf chlorophyll to parameterize light-use-efficiency within a thermal-based carbon, water and energy exchange model. *Remote Sensing of Environment, 115*, 1694–1705.

Huffman, G. J., Adler, R. F., Bolving, D. T., Gu, G., Nelkin, E. J., Hong, Y., ... Stocker, E. F. (2007). The TRMM Multisatellite Precipitation Analysis (TMPA): Quasi-global, multiyear, combined-sensor precipitation estimates at fine scales. *Journal of Hydrometeorology, 8*, 38–55.

Ines, A. V. M., Das, N. N., Hansen, J. W., & Njoku, E. G. (2013). Assimilation of remotely sensed soil moisture and vegetation with a crop simulation model for maize yield prediction. *Remote Sensing of Environment, 138*, 149–164.

van Ittersum, M. K., & Cassman, K. G. (2013). Yield gap analysis — Rationale, methods and applications — Introduction to the special issue. *Field Crops Research, 143*, 1–3.

Jackson, R. D., Idso, S. B., Reginato, R. J., & Pinter, P. J. (1981). Canopy temperature as a crop water stress indicator. *Water Resources Research, 4*, 1133–1138.

Jensen, M. E. (1968). Water consumption by agricultural plants. In T. T. Kozlowski (Ed.), *Water deficits and plant growth* (pp. 1–22). New York: Academic Press.

Johnson, D. M. (2014). An assessment of pre- and within-season remotely sensed variables for forecasting corn and soybean yields in the United States. *Remote Sensing of Environment, 141*, 116–128.

Jonsson, P., & Eklundh, L. (2004). TIMESAT — a program for analyzing time-series of satellite sensor data. *Computers & Geosciences, 30*, 833–845.

Kogan, F. N. (1995). Application of vegetation index and brightness temperature for drought detection. *Advances in Space Research, 15*, 91–100.

Kogan, F. N. (1997). Global drought watch from space. *Bulletin of the American Meteorological Society, 78*, 621–636.

Kogan, F. N., Gitelson, A., Zakarin, E., Spivak, L., & Lebed, L. (2003). AVHRR-based spectral vegetation index for quantitative assessment of vegetation state and productivity: calibration and validation. *Photogrammetric Engineering and Remote Sensing, 69*, 899–906.

Kogan, F. N., Salazar, L., & Roytman, L. (2012). Forecasting crop production using satellite-based vegetation health indices in Kansas, USA. *International Journal of Remote Sensing, 33*, 2798–2814.

Kouadio, L., Newlands, N. K., Davidson, A., Zhang, Y., & Chipanshi, A. (2014). Assessing the performance of MODIS NDVI and EVI for seasonal crop yield forecasting at the ecodistrict scale. *Remote Sensing, 6*, 10193–10214.

Kustas, W. P., & Anderson, M. C. (2009). Advances in thermal infrared remote sensing for land surface modeling. *Agricultural and Forest Meteorology, 149*, 2071–2081.

Launay, M., & Guerif, M. (2005). Assimilating remote sensing data into a crop model to improve predictive performance for spatial applications. *Agriculture, Ecosystems & Environment, 111*, 321–339.

Liu, W. T., & Kogan, F. N. (2002). Monitoring Brazilian soybean production using NOAA/ AVHRR based vegetation condition indices. *International Journal of Remote Sensing, 23*, 1161–1179.

Lobell, D. B. (2013). The use of satellite data for crop yield gap analyses. *Field Crops Research, 143*, 56–64.

Lobell, D. B., Burke, M. B., Tebaldi, C., Mastrandrea, M. D., Falcon, W. P., & Naylor, R. L. (2008). Prioritizing climate change adaption needs for food security in 2030. *Science, 319*, 607–610.

Lobell, D. B., Ortiz-Monasterio, J. I., Addams, C. L., & Asner, G. P. (2002). Soil, climate, and management impacts on regional wheat productivity in Mexico from remote sensing. *Agricultural and Forest Meteorology, 114*, 31–43.

Lobell, D. B., Thau, D., Seifert, C., Engle, E., & Little, B. (2015). A scalable satellite-based crop yield mapper. *Remote Sensing of Environment, 164*, 324–333.

López-Lozano, R., Duveiller, G., Seguini, L., Meroni, M., García-Condado, S., Hooker, J., ... Baruth, B. (2015). Towards regional grain yield forecasting with 1 km-resolution EO biophysical products: Strengths and limitations at pan-European level. *Agricultural and Forest Meteorology, 206*, 12–32.

McVicar, T. R., Roderick, M. L., Donohue, R. J., & Van Niel, T. G. (2012). Less bluster ahead? Ecohydrological implications of global trends of terrestrial near-surface wind speeds. *Ecohydrology (Wiley online), 5*, 381–388.

Mishra, V., Cruise, J. F., Mecikalski, J. R., Hain, C. R., & Anderson, M. C. (2013). A remote-sensing driven tool for estimating crop stress and yields. *Journal of Remote Sensing*, *5*, 3331–3356.

Mkhabela, M. S., Bullock, P., Raj, S., Wang, S., & Yang, Y. (2011). Crop yield forecasting on the Canadian Prairies using MODIS NDVI data. *Agricultural and Forest Meteorology*, *151*, 385–393.

Mkhabela, M. S., Mkhabela, M. S., & Mahinini, N. N. (2005). Early maize yield forecasting in the four agro-ecological regions of Swaziland using NDVI data derived from NOAA's-AVHRR. *Agricultural and Forest Meteorology*, *129*, 1–9.

Moran, M. S. (2003). Thermal infrared measurement as an indicator of plant ecosystem health. In D. A. Quattrochi, & J. Luvall (Eds.), *Thermal remote sensing in land surface processes* (pp. 257–282). Taylor and Francis.

Mozny, M., Tnka, M., Zalud, Z., Hlavinka, P., Nekovar, J., Potop, V., & Virag, M. (2012). Use of a soil moisture network for drought monitoring in the Czech Republic. *Theoretical and Applied Climatology*, *107*, 88–111.

Nearing, G. S., Crow, W. T., Thorp, K. R., Moran, M. S., Reichle, R. H., & Gupta, H. V. (2012). Assimilating remote sensing observations of leaf area index and soil moisture for wheat yield estimates: An observing system simulation experiment. *Water Resources Research*, *48*. http://dx.doi.org/10.1029/2011WR011420.

Otkin, J. A., Anderson, M. C., Hain, C. R., Mladenova, I. E., Basara, J. B., & Svoboda, M. (2013). Examining rapid onset drought development using the thermal infrared based Evaporative Stress Index. *Journal of Hydrometeorology*, *14*, 1057–1074.

Otkin, J. A., Anderson, M. C., Hain, C. R., & Svoboda, M. (2014). Examining the relationship between drought development and rapid changes in the Evaporative Stress Index. *Journal of Hydrometeorology*. http://dx.doi.org/10.1175/JHM-D-13-0110.1.

Prasad, A. K., Chai, L., Singh, R. P., & Kafatos, M. (2005). Crop yield estimation model for Iowa using remote sensing and surface parameters. *International Journal of Applied Earth Observation and Geoinformation*, *9*, 26–33.

Rao, N. H., Sarma, P. B., & Chander, S. (1988). A simple dated water production function for use in irrigated agriculture. *Agricultural Water Management*, *13*, 25–32.

Rembold, F., Atzberger, C., Savin, I., & Rojas, O. (2013). Using low resolution satellite imagery for yield prediction and yield anomaly detection. *Remote Sensing*, *5*, 1704–1733.

Rienecker, M. M., Suarez, M. J., Gelaro, R., Todling, R., Bacmeister, J., Liu, E., ... da Silva, A. (2011). MERRA: NASA's modern-era retrospective analysis for research and applications. *Journal of Climate*, *24*, 3624–3648. http://dx.doi.org/10.1175/JCLI-D-11-00015.1.

Rizzi, R., & Rudorff, B. F. T. (2007). MODIS sensor images associated with an agronomic model to estimate soybean grain yield. *Pesquisa Agropecuária Brasileira*, *42*, 73–80.

Rudorff, B. F. T., & Batista, G. T. (1990). Yield estimation of sugarcane based on agrometeorological–spectral models. *Remote Sensing of Environment*, *33*, 182–192.

Salazar, L., Kogan, F. N., & Roytman, L. (2007). Use of remote sensing data for estimation of winter wheat yield in the United States. *International Journal of Remote Sensing*, *28*, 3795–3811.

Schull, M. A., Anderson, M. C., Houborg, R., Gitelson, A., & Kustas, W. P. (2015). Thermal-based modeling of coupled carbon, water and energy fluxes using nominal light use efficiencies constrained by leaf chlorophyll observations. *Biogeosciences*, *12*, 1151–1523.

Semmens, K. A., Anderson, M. C., Kustas, W. P., Gao, F., Alfieri, J. G., McKee, L., ... Alsina, M. (2015). Monitoring daily evapotranspiration over two California vineyards using Landsat 8 in a multi-sensor data fusion approach. *Remote Sensing of Environment*. http://dx.doi.org/10.1016/j.rse.2015.10.025 (in press).

Sentelhas, P. C., Battisti, R., Câmara, G. M., Farias, J. R., Nendel, C., & Hampf, A. C. (2015). The soybean yield gap in Brazil — Magnitude, causes and possible solutions for sustainable production. *The Journal of Agricultural Science*. http://dx.doi.org/10.1017/S0021859615000313.

Soares, R. M. (2007). Balanco da ferrugem asiatica na safra 2006–07 com base nos numeros do Sistema de Alerta. *Simposio Brasileiro de Ferrugem Asiatica da Soja* (pp. 11–22). London: Embrapa Soja.

Svoboda, M., LeComte, D., Hayes, M., Heim, R., Gleason, K., Angel, J., ... Stephens, S. (2002). The drought monitor. *Bulletin of the American Meteorological Society*, *83*, 1181–1190.

Tadesse, T., Senay, G. B., Berhan, G., Regassa, T., & Beyene, S. (2015). Evaluating a satellite-based seasonal evapotranspiration product and identifying its relationship with other satellite-derived products and crop yield: A case study for Ethiopia. *International Journal of Applied Earth Observation and Geoinformation*, *40*, 39–54.

Teixeira, A. H. d. C., Scherrer-Warren, M., Hernandez, F., Andrade, R., & Leivas, J. (2013). Large-scale water productivity assessments with MODIS images in a changing semi-arid environment: A Brazilian case study. *Remote Sensing*, *5*, 5783–5804.

Unganai, L. S., & Kogan, F. N. (1998). Southern Africa's recent droughts from space. *Remote sensing: Inversion problems and natural hazards* (pp. 507–511).

Wardlow, B. D., Anderson, M. C., & Verdin, J. P. (Eds.). (2012). *Remote sensing for drought: Innovative monitoring approaches.* Boca Raton, FL: CRC Press/Taylor and Francis.

Zaitchik, B. F., Simane, B., Habib, S., Anderson, M. C., Ozdogan, M., & Foltz, J. D. (2012). Building climate resilience in the Blue Nile/Abay Highlands: A role for earth system sciences. *International Journal of Environmental Research and Public Health*, *9*, 435–461.

Zhang, P., Anderson, B., Tan, B., Huang, D., & Myneni, R. B. (2005). Potential monitoring of crop production using a satellite-based Climate-Variability Impact Index. *Agricultural and Forest Meteorology*, *132*, 344–358.

Zwart, S. J., & Bastiaanssen, W. G. M. (2007). SEBAL for detecting spatial variation of water productivity and scope for improvement in eight irrigated wheat systems. *Agricultural Water Management*, *89*, 287–296.